Spring 2016

Experimental evaluations of selected sealants to remediate CO_2 leakage

Aaron Jeffrey Blue

Department:

EXPERIMENTAL EVALUATIONS OF SELECTED SEALANTS TO REMEDIATE CO_2 LEAKAGE

by

AARON JEFFREY BLUE

A THESIS

Presented to the Faculty of the Graduate School of the

MISSOURI UNIVERSITY OF SCIENCE AND TECHNOLOGY

In Partial Fulfillment of the Requirements for the Degree

MASTER OF SCIENCE

in

PETROLEUM ENGINEERING

2016

Approved by

Baojun Bai, Advisor
Runar Nygaard
Ralph Flori

ABSTRACT

Carbon Dioxide (CO_2) sequestration into porous and permeable brine-filled aquifers is seen as one of the most feasible solutions for reducing the amount of greenhouse gases released into the atmosphere from coal-fired power plants. To safely store the CO_2, it must be trapped under an impermeable rock acting as a seal. One of the concerns with CO_2 sequestration is the generation of new fractures or reopening of existing fractures caused by CO_2 injection in the sealing formation. This project evaluates the potential of sealing these fractures by injecting sealing materials into them. These sealing materials need also to stay in place over long term. Therefore the long term thermo-stability of the sealing materials exposed to CO_2 has to be addressed. Four sealing materials have been investigated, at subsurface conditions, to study their ability to effectively seal CO_2 migration through fractures ranging in size from 250 μm up to 1 mm. The four sealant materials were: paraffin wax, silica-based gel, polymer-based gel, and calcium aluminate-based cement. All four materials significantly reduced the fracture permeability. However, the calcium aluminate-based cement was the most effective sealant agent and was the only sealant that was able to withstand the large differential pressure caused by CO_2 or brine injection pressure. Based on the experiments conducted, gels cannot be expected to withstand large pressure differentials in a parallel fracture and therefore the calcium aluminate-based cement is recommended for sealing of fracture widths above half a millimeter. Since cement exposed to CO_2 is subjected to the reaction of carbonation, a potential injection scenario is to inject cement first to create a barrier to differential pressures and then follow with a gel as a secondary seal to create a chemically stable sealing agent exposed to CO_2.

ACKNOWLEDGEMENTS

I would like to thank my advisor, Dr. Baojun Bai, for all of his help during my college career. He has given me the opportunity to work as a research assistant and to be part of his graduate research group.

I would also like to thank Dr. Runar Nygaard. His technical guidance has been vital to the completion of my research projects. He has been an encouraging and supportive mentor in my studies, research, and career. He has given me every opportunity to succeed and has included me in many projects and technical works.

I would also like to thank Dr. Ralph Flori for his time and efforts on my graduate committee.

I would also like to express my thanks and gratitude to the United States Department of Energy for partly funding of this research. This material is based upon work supported by the Department of Energy under Award Number DE-FE0001132.

A special thanks to my wife, Katherine Blue, for her continuous support and encouragement in all of my endeavors.

TABLE OF CONTENTS

LIST OF ILLUSTRATIONS

LIST OF TABLES

1. INTRODUCTION

Coal-fired power plants generate more than 300 GW of electricity, which accounts for over 50% of the electricity in United States, and DOE's Energy Information Agency (EIA) projects these numbers to increase, since coal will likely continue to play a critical role in powering the nation in the foreseeable future (Emily, 2012). Coal-fired power plants emit about 2 billion metric tons of CO_2 annually, and emissions of greenhouse gases like CO_2 have increased over the past century and have been linked to global warming (IPPC, 2007). Injecting carbon dioxide into porous and permeable formations in the subsurface is the most promising method in the near future to reduce CO_2 emissions from stationary sources like coal-fired power plants (IPCC, 2005). Deep saline aquifers, depleted oil and gas fields, and un-minable coal seams are identified as the most likely options for geological formations to store CO_2, and, of these options, saline aquifers have the highest global storage potential (IPPC, 2005).

In view of this massive potential storage capacity, saline aquifers have been identified as very promising geologic storage sites. The storage potential in saline aquifers can be further enhanced by the production of brine out of the aquifer to increase the amount of CO_2 that can be stored, and most importantly, to address the risk of aquifer pressurization and potential CO_2 leakage (Leonenko and Keith, 2008). The risk accompanying aquifer pressurization as a result of CO_2 injection has been addressed, over time by numerous authors (Somayeh et al., 2012; Benjamin et al., 2012; Jens et al., 2012).

CO_2 injected in saline aquifers can be trapped through a combination of one or more chemical and physical processes, which are residual gas, structural, stratigraphic, solubility and mineral trapping mechanisms shown in Table 1.1 (Holtz, 2002; Bachu et al., 2007; Koide et al., 1992).

The most prominent trapping mechanism in any saline aquifer is dependent on the prevailing aquifer properties (anisotropy (heterogeneity), pressure, temperature) and time. These factors, coupled with well completion techniques also affect CO_2 injectivity.

Table 1.1 Characteristics of trapping mechanisms in saline aquifers (Extracted or modified from Alberta Research Council, 2004; Bradshaw et al., 2007).

Trapping mechanism		Characteristics		
		Nature of trapping	Capacity limitation/benefits	Potential size
Geological trapping Reservoir scale (km)	Structural and stratigraphic trapping	Buoyancy within anticline, fold, fault block, pinch-out. CO_2 remains below physical trap.	Without hydraulic system, limited by compression of reservoir fluid. With hydraulic system, displace formation fluid.	Significant
Geochemical trapping Well scale (cm to m)	Residual gas trapping	CO_2 fills interstices between pores of rock grains.	Can equal 15–20% of reservoir volume. Eventually dissolves into formation water	Very large
	Solubility and ionic trapping (Dissolution)	CO_2 migrates through reservoir beneath seal and eventually dissolves into formation water.	CO_2 saturated water may migrate towards the basin center. Limited by CO_2 -water contact and favor highly permeable (vertical) and thick reservoirs	Very large
	Mineral trapping	CO_2 reacts with existing rock to form new stable minerals.	Reaction rate is slow. Precipitation could reduce injectivity. Approaches 'permanent' trapping.	Significant
Hydrodynamic trapping Basin scale (100km)	Migration trapping	CO_2 migrates through reservoir beneath seal, moving with the regional flow system while other trapping mechanisms work.	No physical trap may exist; totally reliant on slow transport mechanism and chemical processes. Can include all other trapping mechanisms along the migration pathway	Very large

Kumar et al. (2002) first recommended that residual gas trapping is an important part of CO_2 trapping mechanism. The mechanism is to trap CO_2 as an immobile phase in the aquifer as a result of the wettability and capillary effects. Residual gas trapping is also a safe trapping mechanism, and it is most effective when the immobile gas is away from the cap rock. This is because CO_2 trapped in pore spaces from which water was displaced (in both cases of with and without brine withdrawal) will remain locked in place (pore space) as a result of the capillary effect and cannot be displaced by imbibition of any fluid. In order for the injected CO_2 to displace the brine initially in the pore space, an injection pressure higher than the prevailing pore pressure will be required. This increases the pore pressure after the CO_2 is injected and the brine displaced, thereby increasing the risk of CO_2 leakage through the cap rock, if this pressure continues to build due to residual trapping. The immobile gas can be kept away from the cap rock by injecting at the bottom of the aquifer and allowing it to rise towards the cap rock by buoyancy. This way, a substantial amount of gas will be trapped during migration upwards (Obi and Blunt, 2006; Juanes et al., 2007; Kumar et al., 2005; Qi et al., 2007). Solubility trapping has been observed to be very low in brine at reservoir conditions; only about 3-5% by mass will

dissolve (Burton et al., 2008). However, the amount of CO_2 that can dissolve in brine is dependent on aquifer temperature, and can be significant (17-29 wt%), while the remaining will exist in the aquifer in super-critical form and will migrate, due to buoyancy, to the top of the aquifer (Bachu et al., 1994; Law and Bachu, 1996). Complete dissolution of CO_2 in brine is estimated to occur between 10,000 to 100,000 years after injection, as estimated from the simulation calculations performed on the Upper Plover Formation in Australia (Ennis-King and Paterson, 2002). The mineral trapping mechanism, which is a form of geochemical reaction, occurs between minerals and aqueous components and between components in the aqueous phase. The kind of mineralization depends primarily on the chemical composition of the aquifer rock, brine salinity, and residence time. Mineral dissolution and precipitation reaction occurs very slowly, taking hundreds to thousands of years, but reactions between aqueous components occurs relatively fast (Lon Nghiem et al., 2009).

Figure 1.1 shows the CO_2 phase diagram. Depending on reservoir temperature and pressure, CO_2 can be in gaseous, super-critical or liquid phase. The CO_2 has a lower density than the formation fluids and will naturally migrate upwards due to buoyancy unless it is contained by a sealing cap rock or a trap, which itself occurs in a complex geological setting and hence creates a complex geometrical model. To successfully inject and store CO_2, a porous and permeable reservoir with a sealing formation above, creating a CO_2 trap, has to be identified.

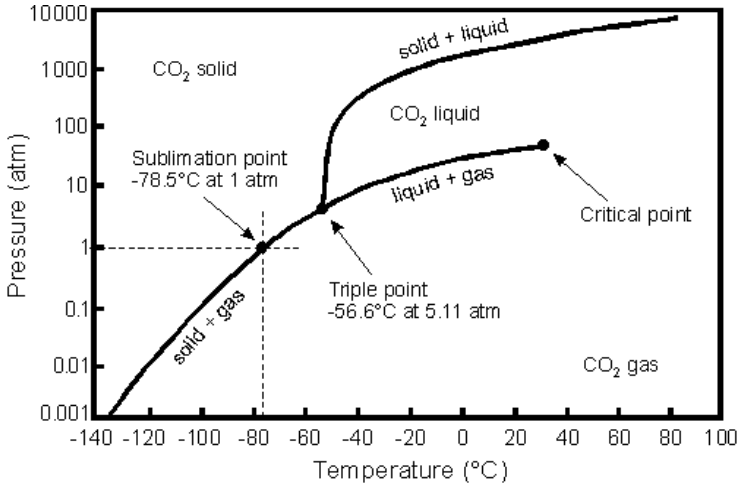

Figure 1.1 CO_2 Phase Diagram (Bachu et al., 1994).

To identify suitable formations to store CO_2, the U.S. has formed 7 regional partnerships to examine subsurface CO_2 disposal in deep formations. The potential CO_2 storage capacity of these geological formations in the Southeast Carbon Sequestration Partnership alone have been estimated to be 2,369 to 9,236 gigatonnes, with saline aquifers accounting for 95% of this storage capacity (Petrusak et al. 2009). The SECARB partnership is comprised of Alabama, Arkansas, Florida, Georgia, Louisiana, Mississippi, North Carolina, South Carolina, Tennessee, Virginia and east Texas. The Plains CO_2 Reduction (PCOR) Partnership, comprised of regions in Canada (Alberta, British Columbia, Manitoba, Saskatchewan) and United States (Iowa, Minnesota, Missouri, Montana, Nebraska, North Dakota, South Dakota, Wisconsin, Wyoming), have also been estimated to have geologic CO_2 storage potential of 242 billion tons; 91% of which is in the saline aquifers (UND-EERC, 2009). However, many states, including the state of Missouri, are located too far away from the deep sedimentary basins and would likely be subject to the highest transportation costs for CO_2 disposal. Therefore, for many utility companies, which are faced with the prospect of federal and state regulation of CO_2 emissions, there is a need to develop an effective and economical means to capture and sequester CO_2 in the proximity of the power plants. Missouri is a member of the Plains CO_2 Reduction (PCOR) Partnership, which is investigating CO_2 transport and injection in the deep formations of the Williston Basin. The state of Missouri lies at the furthest point on the PCOR proposed transportation route and would likely be subject to the highest transportation costs for CO_2 disposal in the Williston Basin. Missouri utility companies are faced with the prospect of federal and state regulation of CO_2 emissions, and the need to develop an effective, economical means to capture and sequester CO_2. Missouri utility companies have expressed an interest in, and have begun to investigate the feasibility of sequestering CO_2 in the Missouri subsurface (City Utilities of Springfield, 2011).

To ensure the public safety, as well as to obtain, carbon credits in a future cap-and trade-system, monitoring and modeling of sequestration projects have to reach a high degree of accuracy. The objective is to reach 99% accuracy in a monitoring and verification program (DOE, 2009). To better predict the long-term fate of injected CO_2 in the subsurface and to quantify potential leakage rates, improved coupled numerical models are needed and further options for mitigation and remediation technologies for potentially

leaking CO_2 need to be developed (Michael et al., 2008). The main leakage risk of CO_2 through a thick, low permeable cap rock is identified to be along existing wells or through faults and fractures. Leakage through wells caused by improper well design or caused by material selection which is not chemically resistant to CO_2 has recently received much attention (Celia 2004, Watson and Bacchu 2007). Several research groups and private companies are actively researching CO_2 resistant cement to seal possible leaking wellbores and to improve future wells to be CO_2 resistant (Min et al., 2011; Liteanu et al., 2011; Kutchko et al., 2007, 2008, Barlet-Gouedard et al., 2006, 2008). However, sealing of faults and fractures has not received the same attention. Michael et al. 2009 identified potential options for mitigation and remediation technologies for leaking CO_2. NETL/DOE (2009) concluded that the mitigation for leakage through preexisting faults and fractures "will be chosen depending on measured and/or anticipated rates of leakage. It can include, but is not limited to decreasing formation pressure and treating the fractures with cement."

To address leakage mitigation, a three-year project was initiated by Missouri University of Science and Technology in partnership with City Utilities of Springfield (Missouri) and funded by the Department of Energy under contract DE-FE0001132. The goal of the project titled "Geomechanical simulation of CO_2 leakage and cap rock remediation" is to investigate CO_2 injection into the Missouri subsurface, study possible caprock leakage of injected CO_2 and develop a technology to remediate the leakage. Materials and methods for stopping leakage through the cap rock will be examined and tested under elevated stresses to simulate in-situ conditions. The approach is designed to be applicable to other types of CO_2 injection sites, including deep saline aquifers.

2. OVERVIEW OF CO_2 LEAKAGE

2.1 PROBLEMS OF CO_2 LEAKAGE

Geological storage of CO_2 can present several hazards if leakage occurs. Ground water contamination is not only costly to fix, but if consumed, can also endanger plants, crops (if irrigation system is using contaminated water), animals, and humans (Bachu *et al*, 2008). Another potential threat is CO_2 migration to the surface where the gas would be dangerous to living organisms that came into contact with it. These health concerns make it even more crucial to carefully plan geological storage locations and have the technology to remediate any leaks as fast as possible.

2.2 LEAKAGE PATHWAYS

CO_2 leakage location can be classified in three different zones: wellbore, near-wellbore and far-wellbore region. For a leak to occur, a leak source, a leakage pathway, and a pressure differential between the reservoir and potential pathway must all be present (Watson *et al*, 2009). For a CO_2 sequestration scenario, a leak source and a pressure differential between the reservoir and a potential pathway are already present. The only one of these factors that can be controlled or remediated is the leakage pathway. Leakage of geologically stored CO_2 can happen in several different ways (Bachu *et al*, 2008; Celia *et al*, 2005) (Figure 2.2.1):

1. Across the cap rock
2. Along the well bore
3. Through natural faults and fractures
4. Through shear fractures
5. Through hydraulic fractures
6. Between permeable zones due to juxtapositions.

CO_2 leakage across the cap rock will most likely occur from the additional stresses added from the injection of the CO_2. This type of leakage can be the most difficult of the three to identify and remediate, as it is difficult to know where the cap rock has the highest stresses and where the cap rock is most likely to fail first. The best way to approach the

challenging task of locating this over-stressed area is to create an accurate earth model of the cap rock section. If a leak is detected, an earth model will allow operators to more easily identify possible areas of failure.

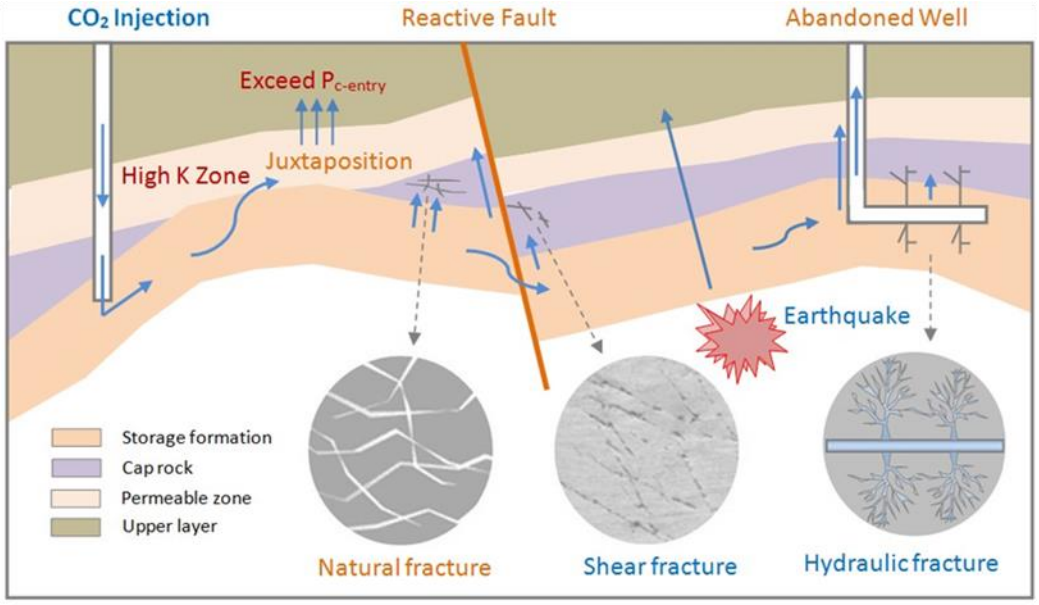

Figure 2.2.1 Possible CO_2 leakage mechanisms in reservoir (Bachu et al, 2008; Celia et al, 2005).

Additionally, an important part of any successful injection project is to avoid any leakage along the wellbore with a well-executed cement placement in the wellbore annulus. Even with a good primary cement sheet initially, the cement integrity might change over the life of the well. One area of active investigation is the fate of cement in CO_2 injection wells caused by chemical instability of Portland cement when it is reacting with CO_2 (Shen et al 1989; Bachu et al 2008) (Kutchko et al, 2007; Barlet-Gouedard et al, 2006). The Portland cement will react with the CO_2 and increase cement porosity when large volumes of CO_2 are present (Kutchko et al, 2007; Barlet-Gouedard et al, 2006). This reaction would intensify at elevated temperatures. Another long-term effect of CO_2 injection is that the injection can impose several stresses on the well casing, the cement boundaries and the formation. Change in thermal stresses caused by cooling or heating may damage the integrity of the wellbore and the cement integrity. Cement failure will create new leakage

pathways for gas to follow. In addition, it is costly to perform work-over operations to squeeze new cement or replace failed casings.

The wellbore can mechanically fail in different modes. Tensile stresses at the casing-cement interface and the cement-rock interface will likely cause de-bonding and opening of fluid pathways at the interface (Figure 2.2.2). Tensile stresses inside the cement or the rock can cause tensile fracturing, if the stresses reach the tensile strength of the material. The tensile strength of steel is so high that tensile failure is not likely to occur in the casing. Shear stresses inside the cement or the rock can cause shear fractures to form, which can also destroy the integrity of the wellbore and act as leakage pathways.

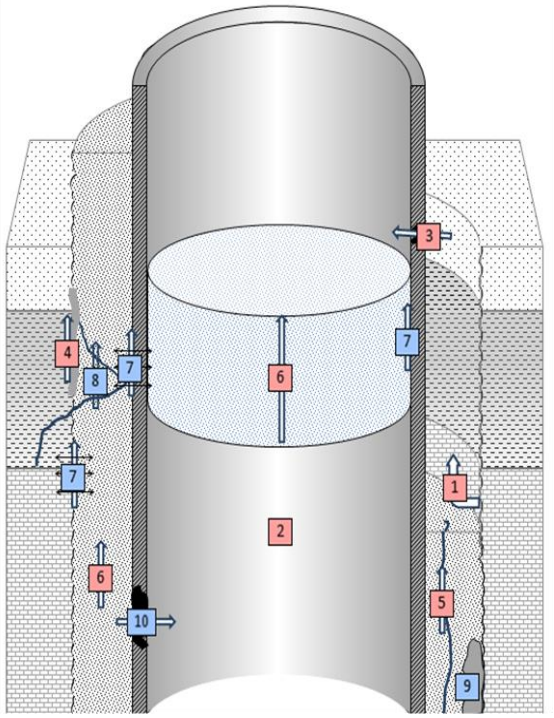

1. Incomplete annular cementing job, does not reach seal layer
2. Lack of cement plug or permanent packer
3. Failure of the casing by burst or collapse
4. Poor bonding caused by mudcake
5. Channeling in the cement
6. Primary permeability in cement sheath or cement plug

Secondary leakage pathways

7. De-bonding due to tensile stress on casing-cement-formation boundaries
8. Fractures in cement and formation
9. Chemical dissolution and carbonation of cement
10. Wear or corrosion of the casing

Figure 2.2.2 Wellbore leakage pathways induced by CO_2 injection loads.

2.3 SELECTION OF CO_2 STORAGE SITE

Currently, the proven CO_2 storage options are depleted oil and gas reservoirs, use of CO_2 in enhanced oil and gas recovery, deep saline formations (both onshore and offshore), and use of CO_2 in enhanced coal bed methane recovery (Flanery *et al*, 2008). While each option has its own criteria for site selection, selecting the best possible CO_2

sequestration location is the crucial first step to minimize leakage risk. For example, if an onshore deep saline formation is being considered, it is crucial that there be a porous, high permeability zone for CO_2 storage that is located below a very low permeability zone that can contain the CO_2. Other factors that will come into play will be wells in the surrounding area and if they are active or abandoned (Barlet-Gouedard *et al*, 2006; Nordbotten *et al*, 2005; Ide *et al*, 2005). If abandoned, then the way in which the well was plugged must be considered.

Selecting the correct plugging materials also plays a large part in preventing leakage. CO_2 injection wells must be able to withstand the corrosive gas and the acids that form once the CO_2 contacts water. Injection wells must be designed with added consideration of casing and cement in a CO_2/carbonic acid rich environment. All casing that will be in contact with the CO_2 must be corrosion resistant.

2.4 REMEDIATION OF LEAKAGE

CO_2 sequestration into saline aquifers and abandoned reservoirs usually leads to increased pore pressure. Increased pore pressure usually results in the possibility of a fracture initiation, which serves as an escape route for otherwise contained CO_2. Once the rock undergoes shear failure and fractures are initiated, their remediation becomes of primary interest. Using coupled fluid flow and geomechanical simulation, the time and location of fracture initiation in the anticline reservoir subjected to CO_2 sequestration can be predicted. Based on the relative location of the failure, different fracture mitigation fluids, such as cement or gel, and remedial strategies, such as injection of retarded cement or drilling of a new remedial well, are investigated to determine the best possible scenario for preventing CO_2 from escaping into upper strata (Figure 2.4.1).

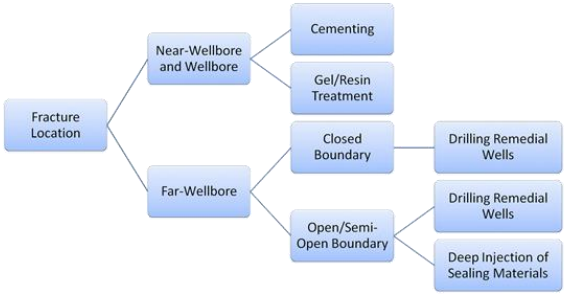

Figure 2.4.1 Fracture Mitigation Work Flow

If the leak is due to casing failure, a possible solution is the use of a pressure-activated sealant. A pressure activated sealant is injected into the leak as a liquid, and the pressure drop along the fracture will cause the sealant to form a plug in the casing crack (Rusch *et al*, 1999). This technology has been field tested and proven several times (Chivvis *et al*, 2009). If the high permeability storage zone or cement is the source of the leakage then one option is to use a polymer gel with cross linker to reduce the permeability (Kabir *et al*, 2001). A study on microgels used for water shutoff in a gas storage well was published showing that in a high to moderate permeability zone (6 Darcys) a large gel (2 μm) was favored (Zaitoun *et al*, 2007). It is still unclear how a gel will perform in a larger fracture. For these cases, cement may be the appropriate choice for plugging the leak. Another similar study was published that addressed CO_2 conformance control in a carbonate media. Results from this study showed that permeability of CO_2 was reduced over 1,500 times when using Alcoflood-935-chromium (III) gel system (Taabbodi *et al*, 2006). There is only information available on testing plugging agents in a porous storage media; there is no information available on the testing of plugging agents in fractures of the cap rock for a CO_2 storage application. In order to solve the problem of CO_2 leakage through cap rock fractures, four different sealant materials were tested: Paraffin Wax, Silica Gel, Polymer Gel, and Calcium Aluminate-based cement. The effectiveness of these materials as fracture sealants was determined by studying them under the following four sub-headings:

- The ability of sealant materials to reduce fracture permeability
- The long term stability of sealing agents
- Time effect on continuous injection of CO_2
- Strength of sealed fractures

3. GEOLOGY OF MISSOURI

3.1 INTRODUCTION

The shallow St. Francois aquifer in the Springfield, MO region is identified as a potential storage unit for shallow CO_2 sequestration from a local coal-fired power plant. This chapter describes the geology of Southwest Missouri where the Lamotte Sandstone, the host rock of the St Francois aquifer, is identified as a potential storage unit (Boongird et al. 2006). Initial characterization of the Lamotte Sandstone identified six facies with varying porosity and permeability and indicated feasibility of CO_2 injection recommending further evaluations. Whole core and thin section analysis were utilized to determine the porosity of the Lamotte formation.

3.2 GEOLOGY OF STUDY AREA

The Springfield, MO site is located in the southwest district on the northeast margin of the Ozark uplift. This occupies a position near the southern edge of the central stable region of the North American craton (Figure 3.2.1).

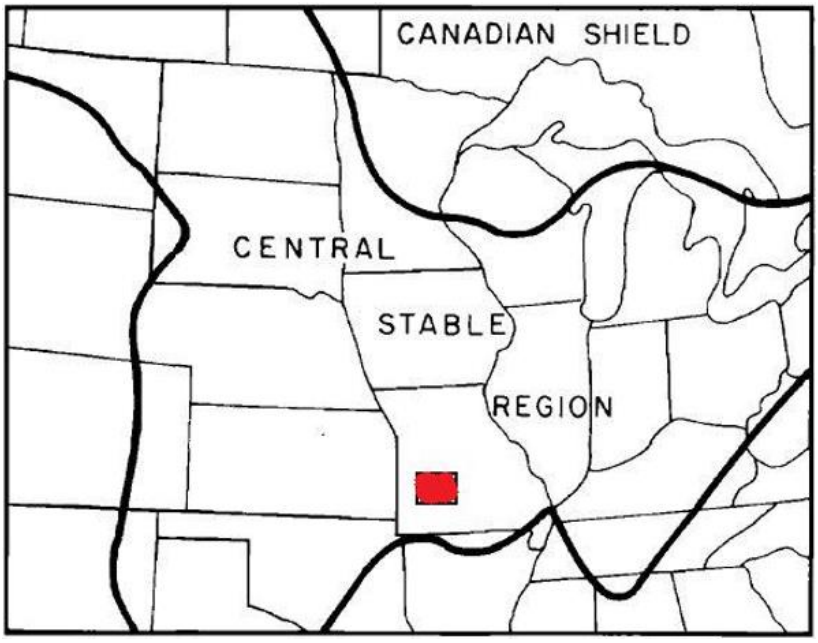

Figure 3.2.1 Central stable region and Ozark Uplift (Snyder and Gerdemann 1968). The red box indicates the target region for the data wellbore site

The sedimentary succession in the Springfield quadrangle is underlain by Precambrian basement. The thickness of the sedimentary strata over the Precambrian ranges from 340m in the northwest to 700m southwest close to the sequestration site. The Precambrian basement is relative to sea level. It is composed mostly of metamorphic rocks (Kisvarsanyi 1975).

The sedimentary sequence of the Springfield site encompasses sediments from the Cretaceous and pre-Cretaceous time periods composed of Cambrian, Ordovician and Silurian units. The deposition of these units occurred as a result of shallow marine transgressions where the bulk of the sediments were derived from the Precambrian sedimentary rocks of the Great Lakes area and deposited in the shallow marine environment around the ancestral St. Francois Mountains (Wallace 1938; Ojakangas 1963).

The Paleozoic sequence consist of the St. Francois aquifer, which comprises the sandstone and conglomerate Lamotte formation in addition to the dolomite, limestone, and sandstone Bonneterre formation. The sealing unit aquitard of the Derby-Doerun and Davis formations consists of mostly shale and dolomite. Above rests the Dolomitic Ozark group which is mainly eroded away in the study area. The aquifer represented by the Lamotte sandstone in which CO_2 is to be injected will occur at depths of approximately 550-700m (Figure 3.3.1).

3.3 LAMOTTE FORMATION

The Lamotte Sandstone is layered on uneven and eroded igneous rock floor which results in wide variation in the thickness of the sandstone. The formation outcrops in northeast St Francois and western Ste. Genevieve and Madison counties. Based on well logs, the greatest thickness recorded is 400ft at Pacific and the lowest being 150ft near Flat River providing an average thickness of about 250ft found in Ste. Genevieve County. The Lamotte Formation extends across Missouri, and has equivalent formations in eastern Kansas stretching north to southern Wisconsin, South Dakota and Minnesota. In the Springfield, MO region, it is expected to consist of arkosic sandstone and/or conglomerate, while the outcrop area consists of minor feldspathic quatzose, glauconitic and dolomitic sandstones. The sandstone is well-bedded, coarse to fine-grained, yellow gray or brown in color, and very friable to lightly cemented. The sand grains are moderately well rounded,

to sub-angular. Shale and conglomerate lenses occur as wavy partings at the top while red hematitic shale sometimes occurs as thin beds in the middle or lower potions, and transitional greenish dolomite beds are common near the top (Thacker and Anderson 1977).

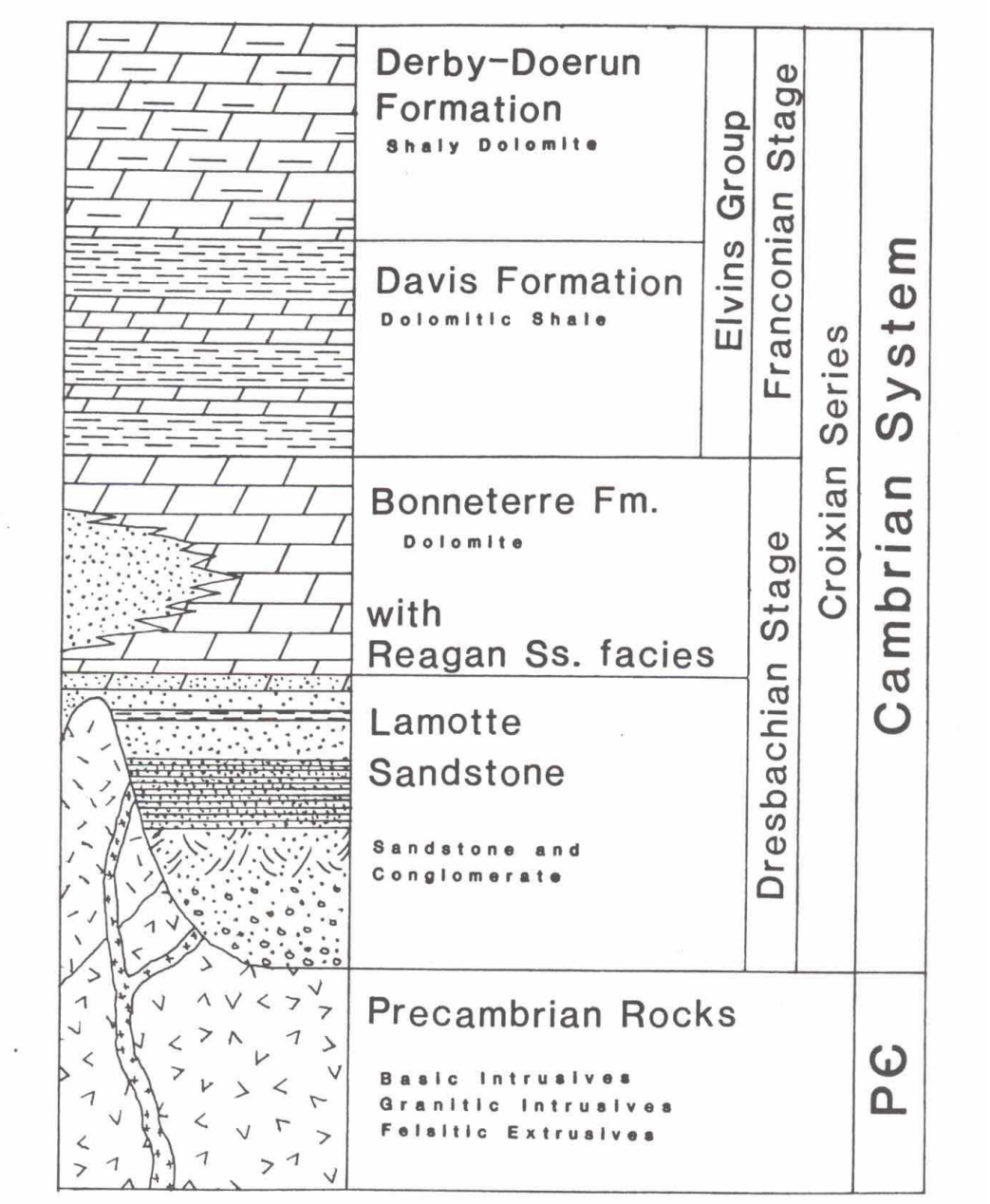

Figure 3.3.1 Composite stratigraphic column of strata (Modified after Houseknecht and Ethridge 1978)

3.4 BONNETERRE FORMATION

Immediately above the Lamotte Sandstone lays the Bonneterre formation. The Bonneterre formation is a complex unit with three layers (lower, middle and upper) strata and constitutes the main lead resource in the state of Missouri. The Bonneterre formation depositional environment is fore reef, reef complex, back reef and shelf facies (Lyle 1977). The Bonneterre formation gradually thickens from the Springfield southwestern region to the southeastern edge of the Precambrian highland (Larson 1977).

3.5 ELVIN'S GROUP

The Elvin's group is divided into Davis and Derby-Doerun Dolomite formations. These formations are expected to form the seal/cap rock due to their limited porosity and permeability, and thus are expected to hold CO_2 in place after injection.

The Davis formation is distinguishable from the units above and below it by its high shale content. The contact with the underlying Bonneterre formation is believed to be unconformable. The Bonneterre consists of interbedded green shales, sandy and silty limestones and calcareous siltstones/dolomite. Flat pebble conglomerates exist in the formation and fine grains of glauconite occur throughout. A greater amount of clastic materials and glauconitic occur in the lower portion. The conformable contact with the Derby – Doerun formation is not clearly defined but tends to occur where the green Davis shale is replaced by brown Derby-Doerun shale. Intertonguing of the Davis and Derby-Doerun lithologies occur (Thacker and Anderson 1977).

The Derby-Doerun formation is divided into two distinct lithological units. Lower Derby-Doerun consists of thin, irregularly bedded, and fine to medium crystalline argillaceous dolomite. Wavy, brown shale and thin beds are predominant. This unit is silty and contains glauconite grains with massive amounts of clastic material. The upper Derby-Doerun is massively bedded, fine to medium crystalline, burrowed and contains argillaceous dolomite. The formation is sometimes calcernitic with beds of oolites. Stromatolites are present. The contact between the lower and upper Derby-Doerun is marked by sharp decrease in clastic material such as shale and silt-sized quartz grains The contact between the Derby-Doerun and the Potosi Dolomite is poorly defined and is likely gradational (Thacker and Anderson 1977).

3.6 OUTCROP SAMPLING

Due to the uplift in the lithology in eastern Missouri, there are outcroppings around Park Hills, Missouri that are located thousands of feet below the surface in the southwest corner of the state. Therefore, all core samples were drilled from outcroppings that were collected from the following locations (Table 3.6.1 and Figure 3.6.1):

Table 3.6.1 Outcropping Locations

Formation	Location	Elevation [ft]
Derby Doe Run	N 37° 49.893'; W 090° 31.644'	899
Davis	N 37° 51.825'; W 090° 33.778'	800
Bonneterre	N 37° 49.735'; W 090° 40.480'	829
Lamotte	N 37° 48.733'; W 090° 34.789'	896

Figure 3.6.1 Davis Shale Outcropping

The fairly consistent lithology throughout Missouri consists of the permeable and porous Lamotte Sandstone that sets below the three low-permeable formations of the Bonne Terre Dolomite, Davis Shale, and Derby Doe Run Shaly Dolomite (listed from bottom to top in Table 3.6.1).

4. EXPERIMENTAL APPROACH

4.1 INTRODUCTION

The main concerns with CO_2 sequestration is the generation of fractures or fracture reactivation caused by CO_2 injection in the cap rock. To seal fractures and faults, a sealing material can be injected but it has to have certain properties. The sealing material needs to withstand the differential pressure caused by the elevated CO_2 pressure in the reservoir, and it also needs to be stable and stay in place in the fracture over a long time period. Therefore, the long-term stability of the sealing materials exposed to CO_2 has to be addressed from a pressure differential point of view, as well as chemical stability when exposed to CO_2. The results are a conclusion of the project objective to develop methodologies to simulate cap rock leakage, to select cap rock sealants, and simulate the success of remediation of leakage paths. The following tests were conducted:

(1) Rheology measurements to characterize strength of sealants described in Chapter 4.3
(2) Core flooding tests on intact and fractured cores to investigate fracture permeability reduction described in Chapter 4.4
(3) The bottle test method to evaluate the stability of sealing materials described in Chapter 5.4
(4) Modified direct shear tests to evaluate fracture permeability change on fracture movement described in Chapter 5.5
(5) Hydraulic fracturing cell to determine sealed-fracture strength described in Chapter 5.8

4.2 DESCRIPTION OF SEALANT MATERIALS

Silica Gel formulations included Silicate (7%), Calcium Chloride (6-10%), and distilled water (87-83%). Powdered Silicate was obtained from Unimin Specialty Minerals, Inc. in Tamms, IL.

Marcit GT-955 Polymer and Chromic Acetate Crosslinker were obtained from Gel Technologies Corporation in Midland, TX. The GT-955 Polymer is an anionic water-soluble polymer that crosslinks when in the presence of the 11.2% active Cr^{+3}.

Fondu micro-cement was obtained from Kerneos Inc. in Chesapeake, VA. Excellent resistance to a wide range of chemicals. This cement is ideal for high temperature applications and has low porosity. The full cure time is similar to Portland cement but initially hardens at a faster rate. This rapid initial hardening allows for return to service in as little as 6 hours after mixing. The formulation for Fondu is listed in Table 4.2.1.

Table 4.2.1 Fondu Formulation

Component	**Specification Limit**
Al_2O_3	> 37%
CaO	< 41%
SiO_2	< 6%
$Fe_2O_3 + FeO_3$	< 18.5%
MgO	< 1.5%
TiO_2	< 4%
S (as sulphide ions)	< 0.1%
Cl (as chloride ions)	< 0.1%
$Na_2O + 0.659\ K_20$	< 0.1%

Paraffin wax was obtained locally from a Lowe's retail store. Paraffin wax consists of a mixture of heavy hydrocarbon molecules.

4.3 RHEOLOGY TESTS

To evaluate the strength of the gel (i.e. elastic shear strength moduli - G') a HAAKE RheoScope was used. The oscillation time sweep curve model was selected for the measurement; it represents the storage and loss moduli logarithmically in Pascal (Pa) as a function of time in seconds. The frequency was set at 1.0 Hz. A controlled stress (CS) mode was chosen because the selected stress value had to be in the linear

viscoelastic range. The stress applied to the gel was 1.0 Pa to ensure that the gel strain and stress had a linear relationship during measurement. A PP35 Ti Po LO2 016 sensor was used, and a gap of 0.2 mm between the sensor and the plate holding the gel sample was used. For each sample, storage modulus readings were taken every 30 seconds for three minutes.

4.4 CORE FLOODING TESTS

This chapter presents the preparation, apparatus and procedure to measure the change in fracture permeability before and after sealant was injected. One-inch diameter cores were drilled out of the Lamotte Sandstone, Bonneterre Limestone, Davis Shale and Derby-Doe Run Shaly Dolomite outcroppings. First, the intact core permeability was measured in the high-pressure, high-temperature core flooding apparatus developed in this project. Secondly, fractured cores were tested before and after sealant were injected.

4.5 SAMPLE PREPARATION

The fairly consistent lithology throughout Missouri consists of the permeable and porous Lamotte Sandstone that sets below the three low permeable formations of the Bonne Terre Dolomite, Davis Shale, and Derby Doe Run Shaly Dolomite (listed from bottom to top).

The first part of testing would be to evaluate the efficiency of the plugging agents and all four formations with a standard fracture width of 0.5 mm. The second round of tests would evaluate the plugging agents' efficiency to reduce flow through fractures of different widths using the Lamotte Sandstone. Fracture widths tested are 0.25 mm, 0.5 mm, and 1.0 mm.

Figure 4.5.1 shows how the artificially fractured core is created. First, the core is cut in half with a rock saw, before a grinding wheel is used to create an artificial fracture. The saw blade used to cut intact core in half is 1.5 mm thick. The amount of material removed from the average core due to cutting is less than 0.04 cm^3 (<.04% of total initial volume). This surface area/volume decrease will translate into an increase in differential pressure. However, if the permeability was calculated using a constant area of the injection face, then the difference in permeability of a 6.8 md core sample with a length

of 5.715 cm and a diameter of 5.065 cm would be <0.003 md. This permeability difference is negligible for this study, and a constant area was used in the calculations of the cores.

In order to have control of the fracture location, fracture width, and fracture length, a new method had to be developed in order to make uniform fractures. The first step of this process was securing an "L-shaped" block to the diamond saw fence (Figure 4.5.2).

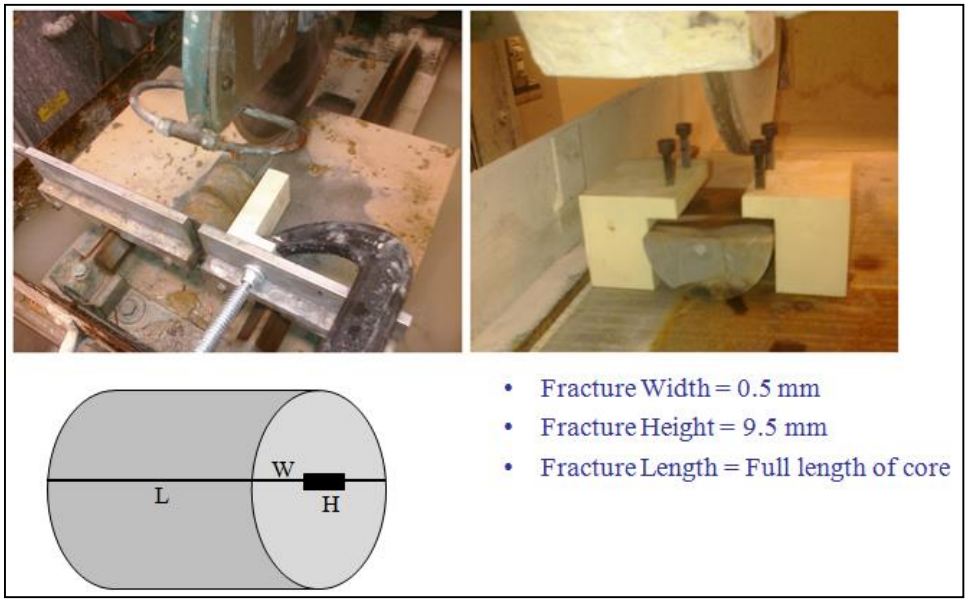

Figure 4.5.1 Artificially Fractured Core

Figure 4.5.2 Split Sample

The block had to be placed so that the cut would produce two nearly identical pieces. Once the core was made into two pieces, one of those pieces was selected for grinding of the fracture to the predetermined fracture width. The selected core half was secured to the magnetic grinding table by use of metal “L-shaped” block with set screws (Figure 4.5.3).

Figure 4.5.3 Grinding Desired Fracture Width

The set screws where adjusted until the core was level to the grinding wheel. Then the grinding wheel was zeroed out to the elevation of the top of the core. The grinding wheel was then lowered to the desired fracture width (the elevation controls are accurate to +/-0.004”) and the wheel was fed across the entire core length. Digital calipers were used to ensure desired depth had been reached. The two halves of the core are then re-aligned and clamped together. Epoxy is then placed on the outside of the core to help hold the core together during transport and also during testing (Figure 4.5.4).

Figure 4.5.4 Fractured core held together with epoxy

The epoxy used has a high viscosity to prevent unintended migration of epoxy during curing. During the application of the epoxy, extra care is taken to ensure none of the material is placed between the two halves or on the injection or outlet faces (Figure 4.5.5).

Figure 4.5.5 Fractured core front view

5. METHODOLOGY AND EXPERIMENTAL PROCEDURE

The laboratory set up is shown in Figures 5.0.1 and 5.0.2. A syringe pump is used to fill the transfer cylinders (upright steel cylinders in Figure 5.0.2) with the test fluid before being injected into the core holder (horizontal stainless steel cylinder in Figure 5.0.2). The pressure drop is measured over the core holder, and the gas and fluids are separated in the separating beaker (Figure 5.0.2). Outlet gas flow is measured, and outlet liquid flow is diverted to either a 0.25 lb scale or a 5 lb scale depending on expected flow rate. The core holder is mounted inside a constant temperature cabin to ensure that fluid density and viscosity are not varied due to temperature changes. The apparatus has capabilities for elevated temperatures which have not been used in these experiments. Carbon dioxide was used for the gas permeability testing and 4% wt of potassium chloride (KCl) brine was used for the liquid permeability testing. A confining pressure of 1500 psi was used and flow rates ranged from 0.5-3.0 mL/min for the liquid permeability tests. Flow rates of the gas permeability tests ranged from 0.5-5.0 mL/min.

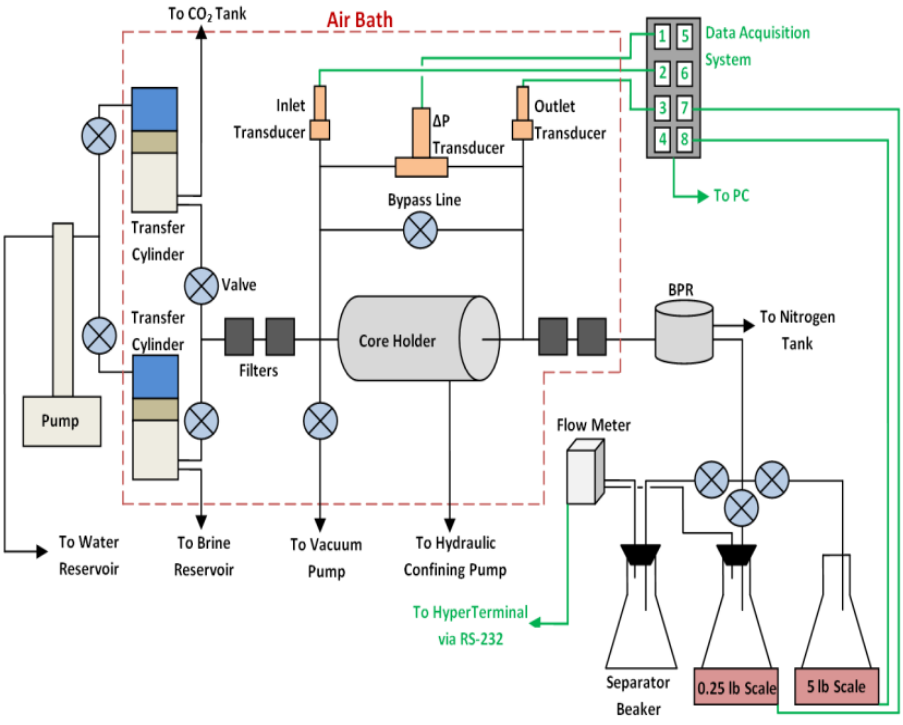

Figure 5.0.1 Schematics of the core flooding apparatus for intact and fracture permeability tests.

After the intact permeability was measured the core was cut into two half as shown in Figure 4.5.2. A grinder wheel was used to create an artificial fracture of 9.5 mm height and 0.5 mm width along the whole core length (Figure 4.5.3). The core was then inserted back into the core holder and fracture permeability was measured with flow rate of 1.0 to 2.0 mL/min.

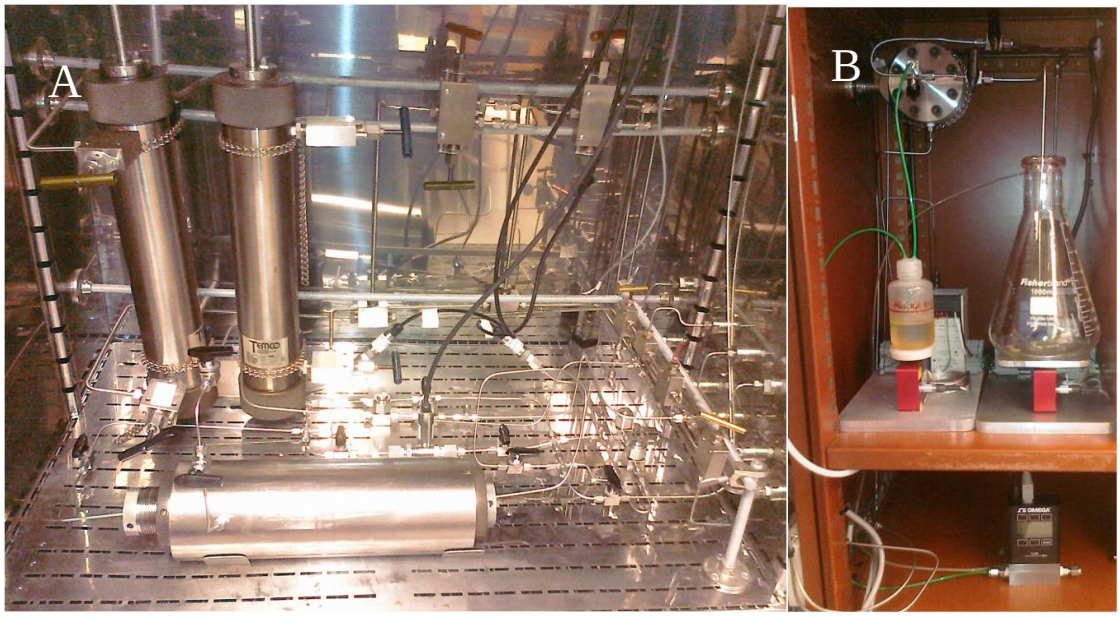

Figure 5.0.2 Core Flooding System Setup

A) Core holder and transfer cylinders located inside the constant temperature cabinet. B) Gas/liquid separation beakers are shown with liquid weight scale and gas mass flowmeter.

5.1 PARAFFIN WAX

To inject the paraffin wax plugging agent, a special wax injection system and procedure was developed (Figure 5.1.1). First, cores were vacuumed using the core flooding system and then saturated with 4% KCl brine before CO_2 was injected until no more brine flowed out. Then, paraffin wax was heated until the temperature reached 275 ^{o}F and the core was placed in the accumulator, which was filled with paraffin wax until the core was completely submerged. The accumulator was pressurized with 100 psi of CO_2 and the wax was cooled for 12 hours before being removed from the actuator. Finally,

excess paraffin wax was removed from the core and the injection and discharge faces were scrapped free of any remaining wax.

1. Vacuum core using the core flooding system
2. Saturate vacuumed core with 4% KCl Brine
3. Inject CO_2 through the KCl saturated core until no more brine flows out
4. Remove core from core holder
5. Heat paraffin wax until temperature reaches 275 ºF
6. Place core in accumulator
7. Fill accumulator with paraffin wax until core is completely submerged by 2inches of wax
8. Tighten top cap onto the accumulator and pressurize the system with 100 psi of CO_2
9. Shut the valve and let the wax cool for 12 hours before removing
10. Remove core from accumulator
11. Remove excess paraffin wax from core and scrape the injection and discharge faces free of any remaining wax.

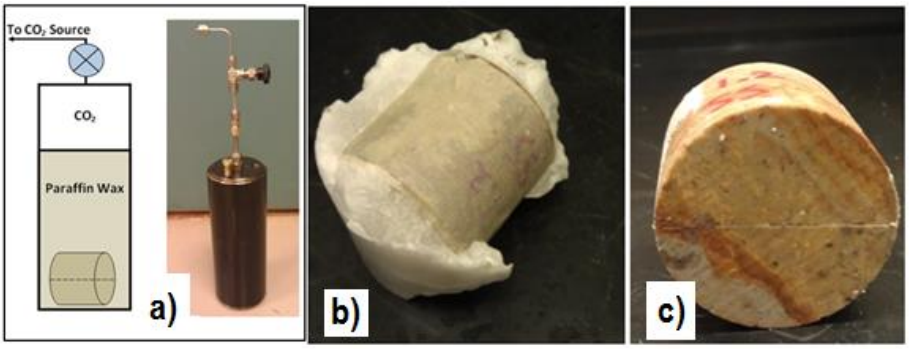

Figure 5.1.1 Paraffin Wax
(a) Paraffin Wax Injection System
(b) Fractured core removed from paraffin wax injection system with excess wax
(c) Fractured core with excess paraffin wax removed

5.2 POLYMERS AND SILICA GELS

To obtain consistent polymer and silica gel plugging agent injection results, the apparatus and procedure had to be modified from the previous experiments. Figure 5.2.1 shows the modified injection caps, which were used with the gel injection system. These

injection caps were more effective injecting the sealant into the fractured core than the traditional distribution cap. The new injection caps only allow injection from a 1/8" diameter hole in the cap, which forced the flow into the fracture and more repeatable sealing fracture permeabilities were measured. The reason for the improved repeatability was that the wax plugged up the distribution channels in the distribution caps, which lead to a less effective injection into the fractures and thereby reduced the amount of sealant that was transferred into the fractures.

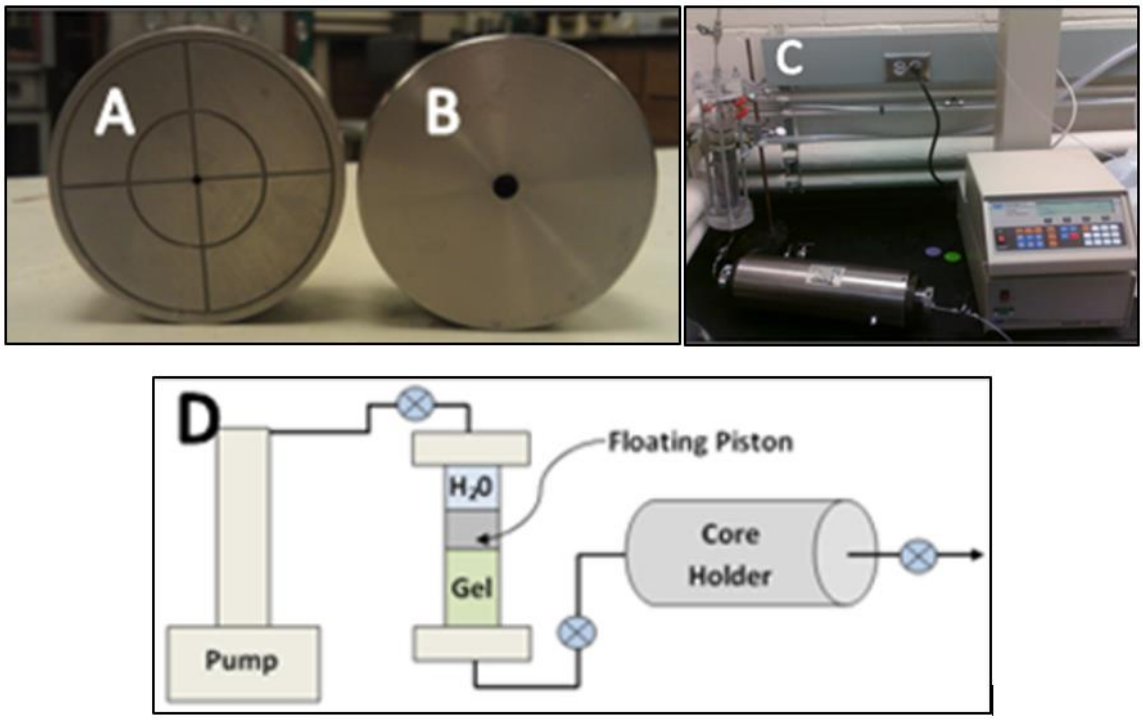

Figure 5.2.1 Gel Injection System
A) Distribution cap
B) Injection cap
C) Picture of gel injection system
D) Schematics of gel injection system

To prepare the experiments for the injection sealant, the core was subjected to a vacuum by using the core flooding system. Then the vacuumed core was saturated with 4% KCl brine before CO_2 was injected through the KCl saturated core until no more brine came out the next step was to hookup the core holder to the injection system. The polymer or silica gel was injected through the fractured core at 100 psi until a steady stream of

polymer was discharged from the core holder. The outlet valve was closed on the outlet line, while keeping the pump running at 100 psi for 15 minutes. The valve was closed on the injection line, and the core was exposed to 150 ºF for 12 hours. Then the core holder was removed from the injection system, and the plugging agent was allowed to set-up. The injection cap was removed, and the core surface was cleaned from any excess polymer. The core holder was reassembled with the distribution plugs.

Two types of gel systems were tested: a silicate-based gel, and a Marcit polymer-based gel. To decide the concentrations of silica gels and polymer gels, the gel strength was measured using a rheoscope. Table 5.2.1 gives the different gel composition prepared for the testing.

Table 5.2.1 Silica gel and Marcit polymer concentrations

Gel	Silicate	Calcium Chloride	Distilled Water	Polymer Concentration [ppm]	Polymer to Crosslinker Ratio
S1	7%	6%	87%		
S2	7%	8%	85%		
S3	7%	10%	83%		
M1				4000	44:1
M2				5500	55:1
M3				7000	55:1
M4				8500	66:1

5.3 CALCIUM ALUMINATE-BASED CEMENT

The fourth type of plugging agent used was micro-cement, called Fondu, used to seal off the micro-annulus in wells. To find the correct cement concentration, the plastic viscosity and yield points for multiple concentrations were measured at time intervals of 5, 15 and 30 minutes by using a Fann 35 viscometer (Table 5.3.1). It is desirable to have the lowest water concentration possible and still allow for fairly easy flow. Low water concentration is desirable since it will reduce the potential for shrinkage during the cement curing process.

Table 5.3.1 Cement plastic and yield point selection

	% Water	300 RPM	600 RPM	Plastic viscosity (cP)	Yield Point (lb/100ft^2)
5 minutes	65%	4.5	10	5.5	4.5
	60%	6.5	12	5.5	6.5
	55%	7	13.5	6.5	7
	50%	7	14	7	7
	45%	10.5	19	8.5	10.5
	40%	13	27	14	13
	35%	21	46	25	21
	30%	73	139	66	73
15 minutes	65%	4	9.5	5.5	4
	60%	5	10	5	5
	55%	5.5	11.5	6	5.5
	50%	7	14	7	7
	45%	11	19.5	8.5	11
	40%	14	27	13	14
	35%	20.5	44	23.5	20.5
	30%	57	108	51	57
30 minutes	65%	4	9	5	4
	60%	5	10	5	5
	55%	6	12	6	6
	50%	8	15	7	8
	45%	13	21	8	13
	40%	16.5	29	12.5	16.5
	35%	22.5	44	21.5	22.5
	30%	N/A	N/A	N/A	N/A

Based on the initial screening of water concentrations, a water content of 45% was selected as the sample with lowest water content and acceptable plastic viscosity and yield points (Table 5.3.1). The shrinkage of the 45% water content cement mixture was checked and gave an acceptable shrinkage of 1.4% (Table 5.3.2).

Table 5.3.2 Cement shrinkage results

	45% Water, 55% Micro cement Fondu				
	Volume Initial [mL]	**Tube Diameter [cm]**	**ΔL [cm]**	**Shrinkage Volume [mL]**	**Shrinkage**
Open	40	2.656	0.101	0.560	1.40%
Closed	40	2.656	0.133	0.737	1.84%

The Polymer/Silica Injection System could not be used for cement injection. The floating piston would become seized in the cylinder. Also, the design of the core holder would have caused the core sample to become cemented to the rubber sleeve making the core difficult to remove. The Paraffin Wax Injection System would not work either due to the fact that the cement would bind to the walls of the accumulator and prevent the sample from sliding out easily. In order to avoid these issues, a different injection procedure had to be used.

- Determine the quantity of dry Fondu micro-cement and water required
- Weigh out the required components
- Use a overhead mixer to stir the water and slowly add in the dry Fondu micro-cement
- Mix the cement for 10 minutes
- Apply mixed cement on cut cores and clamp together (Figure 5.3.1)

Figure 5.3.1 Cement Fondu Preparation

Each sample that was used for a core flooding test went through the following procedure. First the sample drilled from an outcropping. The cylinder were then cut to desired length. Then the rough cut faces of the cores were smoothed down by use of a grinding wheel. After the core has reached the desired dimesions, the core is placed in an oven for 6 hours at 220 °F. The cores are then removed from the oven and the core length, diameter, and weight are recorded.

The samples that are selected for non-fractured KCl permeability testing went through the following procedure. First the sample is placed into a vacuum system for 12-24 hours. The core is saturated with a 4% KCl brine fluid. Saturated core weight is recorded and effective porosity of the core is calaculated using a known brine density. The core is now ready to be place into the core flooding core holder. 4% KCl is injected at a constant rate until the injection and outlet pressures stabilize. Permeability is then calculated.

To test non-fractured CO_2 permeability and KCl brine residual saturation the following procedure was followed. CO_2 was injected through the KCl saturated core until no more brine flows out. This was confirmed by monitoring the liquid scale on the outlet line. CO_2 permeability was then calculated. The sample was then removed from the core holder and the weight is recorded. KCl residual saturation was then calculated using known brine density.

To generate an artificially made fracture into the core the following procedure was followed. The core was cut in half along the long axis. Then a grinding wheel was used to cut the desired fracture width (0.25, 0.5, and 1.0 mm). The core was then placed in an oven for 6 hours at 220^{o}F to remove any water saturation that occurred during the cutting/grinding process. Resin is then applied to the core to hold the two halves together.

The core flooding test matrix is listed in Table 5.3.3. Lamotte sandstone samples underwent testing with Marcit gel, paraffin wax, silica gel, and Fondu micro-cement with fracture sizes ranging from 0 mm to 1 mm. The Bonneterre samples were tested with Marcit gel with fracture sizes ranging from 0 mm to 0.5 mm. The Davis and Derby Doe Run samples were tested with Marcit gel and Fondu micro-cement with fracture sizes ranging from 0 mm to 0.5 mm.

Table 5.3.3 Core Flooding Test Matrix

Core #	Exp #	Core Type	Inj Fluid	Plugging Agent	Frac Width [mm]
1.1	1	Lamotte	Brine		0
	2		CO_2		
	3		Brine	MARCIT Gel	0.50
	4		CO_2		
1.2	5	Lamotte	Brine		0
	6		CO_2		
	7		Brine	Paraffin Wax	0.50
	8		CO_2		
1.3	9	Lamotte	Brine		0
	10		CO_2		
	11		Brine	Silica Gel	0.50
	12		CO_2		
1.4	13	Lamotte	Brine		0
	14		CO_2		
	15		Brine	MARCIT Gel	0.25
	16		CO_2		
1.5	17	Lamotte	Brine		0
	18		CO_2		
	19		Brine	MARCIT Gel	1.00
	20		CO_2		
1.6	21	Lamotte	Brine		0
	22		CO_2		
	23		Brine	Foundu Cement	1.00
	24		CO_2		

Core #	Exp #	Core Type	Inj Fluid	Plugging Agent	Frac Width [mm]
2.1	25	Bonne Terre	Brine		0
	26		CO_2		
	27		Brine	MARCIT Gel	0.50
	28		CO_2		
3.1	29	Davis	Brine		0
	30		CO_2		
	31		Brine	MARCIT Gel	0.50
	32		CO_2		
4.1	33	Derby Doe Run	Brine		0
	34		CO_2		
	35		Brine	MARCIT Gel	0.50
	36		CO_2		
3.2	37	Davis	Brine		0
	38		CO_2		
	39		Brine	Foundu Cement	0.50
	40		CO_2		
4.2	41	Derby Doe Run	Brine		0
	42		CO_2		
	43		Brine	Foundu Cement	0.50
	44		CO_2		

5.4 LONG TERM THERMO-STABILITY OF POLYMER GELS

To ensure CO_2 is stored safely over the long-term in the reservoir, potential sealant materials need to be stable when exposed to CO_2. Marcit polymers crosslinked with Chrome acetate was investigated. All reagents were used as received. All solutions were prepared in deionized water. The reaction tube was specially designed to withstand high pressures and high temperatures (Figure 5.4.1).

Figure 5.4.1 Experimental setup for long-term stability testing

The laboratory set up was made with high density polyethylene, which can withstand elevated temperatures of up to 150^{o}C and is chemically inert.

Gels were prepared by first making 1% (10,000 ppm) polymer solution by dissolving a measured amount of polymer in deionized water (Table 5.4.1).

Table 5.4.1 Gel strengths for the different Set 1 samples sealed in CO_2

Sample	Gel strength Code
4000 ppm	C
5500 ppm	D
7000 ppm	F
8500 ppm	G

From this, four different polymer concentrations of 4000 ppm, 5500 ppm, 7000 ppm and 8500 ppm were prepared by dilution. The corresponding chrome acetate volume was added and stirred for about 20 seconds. Three different sets of four samples were prepared. The first set was placed in oven for 2 hours at 65^{o}C for gel formation to occur. After gelation, samples were vacuumed to about 1 atm, and CO_2 was injected to 10 atm. Set 2 samples were similarly placed in oven for 2 hours at 65^{o}C. After gelation, no CO_2 was injected into these. In Set 3 samples, CO_2 was injected before samples were placed in oven. All three sets were kept at room temperature for 7 months and evaluated regularly for changes in gel strength and viscosity.

A semi-quantitative bottle test method to measure gel strength developed by Sydansk (1988) was employed. By this method, a particular letter code from A to J was assigned to a particular gel strength (Table 5.4.2). The codes range from no detectable gel formed (A) to a ringing rigid gel (J). Herein, the CO_2 sealed gels in the bottle tubes were inverted, and the gel strength was measured as a function of time. Monthly, samples were consistently inspected by visual observation for changes in gel flowability. By inverting the bottles during each reading, the gel's flow characteristics under the influence of gravity were observed.

Table 5.4.2 Sydansk gel-strength codes (Sydansk, 1988).

Gel Strength Code		Description
A	No detectable gel formed	The gel appears to have the same fluidity as the original polymer.
B	Highly flowing gel	The gel appears to be only slightly more viscous than the initial polymer solution.
C	Flowing gel	Most of the obviously detectable gel flows upon inversion.
D	Moderately flowing gel	A small portion (5 to 15%) of the gel does not flow readily upon inversion.
E	Barely flowing gel	The gel can barely flow to the bottle top, and/or a significant portion (>15%) of the gel does not flow upon inversion.
F	Highly deformable non-flowing gel	The gel does not flow to the bottle top upon inversion (reaches a point just short of bottle top).
G	Moderately deformable non-flowing gel	The gel flows approximately half the way down the bottle upon inversion.
H	Slightly deformable non-flowing gel	Only the gel surface slightly deforms upon inversion.
I	Rigid gel	There is no surface deformation upon inversion; gel is stable and clear.
J	Ringing rigid gel	A tuning-fork like mechanical vibration can be felt after tapping the bottle.

5.5 SHEAR APPARATUS

The shear strength of the sealed fractures was tested using a modified GCTS direct shear apparatus (Figure 5.5.1). The apparatus is able to test a wide range of rock mechanics specimen to determine the shear strength of the fractures in the rocks.

The system works on the application of normal load and horizontal shear load. The normal and shear deformations were monitored using either linear variable differential transducers (LVDTs) or dial gauges. At the end of the experiment, a shear stress vs time graph was generated from which peak and residual shear strength were determined. The experimental set up was modified based on the design from Gutierrez et al, (2000) so fluid could be injected in the middle of the fracture during the shearing phase and permeability can be determined. After the experiment, the cemented rock inside the shear ring was carefully taken out using a hammer and chisel.

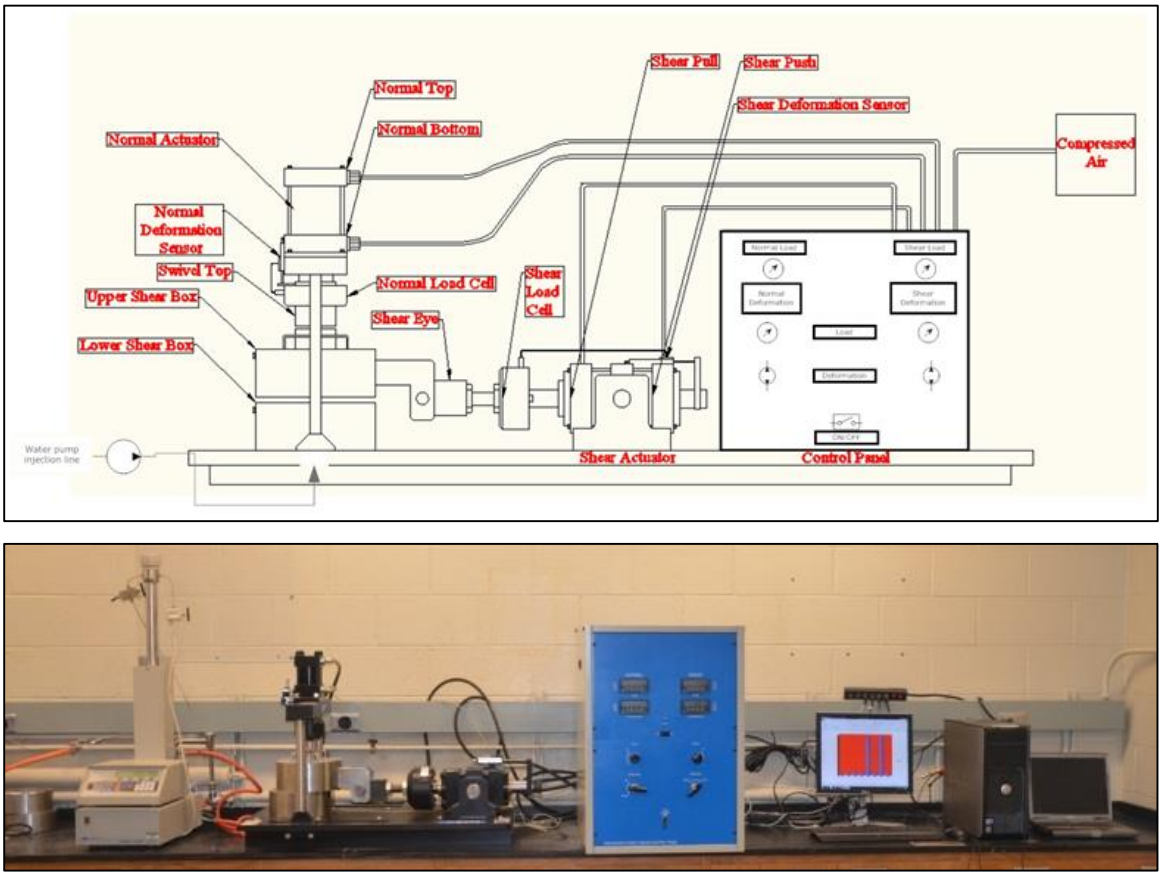

Figure 5.5.1 Direct shear apparatus

Geological storage projects of CO_2 are designed to maintain secure storage for thousands of years. Potential leakage of injected CO_2 from the reservoir to the surface is caused by the reactivation of pre-existing faults and fractures which is caused by the change in the state of stresses and the pore pressure. To avoid damage to the reservoir sealant materials, ensure fault stability and validate maximum sustainable pore pressure, a geomechanical characterization which refers to the assessment of the in-situ stress, elastic properties and, rock strength of the rock helps to determine the effectiveness of the sealant material to continuously seal the cap rock during periods of stress and pore pressure changes. Thus, the integrity of the storage capacity of the reservoir during and after injection of CO_2 in underground formations is maintained.

In this study a direct shear apparatus was assembled in order to determine the direct shear strengths of the rock. Mohr-Coulomb failure criteria, slip tendency parameters and

joint roughness coefficient were used to determine the chances of the reactivation of pre-existing faults and fractures in the caprock and the reservoir rock. Three experiments were run:

- Fractured rocks with no sealant material (that is air)
- Fractured rocks sealed with micro-cement
- Fractured rocks sealed with Marcit gel

Fault activation is basically activation of pre-existing faults which may occur whenever the shear stress acting on the fracture plain exceeds the Mohr-Coulomb failure criteria represented by Equation 1, where τ_s is the shear stress, φ is the friction angle, c is the cohesion, and σ_n is the normal stress. The practical application of this equation is that whenever the left side exceeds the right side, the fault will slip creating a possible leakage pathway for CO_2.

$$|\tau_s| \geq c + \sigma_n tan\varphi \quad (1)$$

The essence of this study is to ascertain that, when the fault slips and reactivates the fracture, the sealant material will also move accordingly to occupy this new fracture, thereby continuously sealing the fracture and maintaining a zero change in fracture permeability. To achieve this, we designed our experiment to simultaneously measure both the shear strength and the variation in permeability of the sealed fracture with shearing.

5.6 SAMPLE PREPARATION FOR DIRECT SHEAR TEST

The rock used for mechanical testing in this research was cored from the outcroppings found in the region under consideration for CO_2 sequestration. The samples were prepared by cutting the source rock using the rock saw in the department. Cubical test specimen of dimension 4” in length, 4” in width and 5” in height were used for the test. Rock boulders were cut into cube shapes using the rock saw. Fractures were created in the rock samples by cutting the cubic rock boulders into equal halves using a rock saw. Rock sample after creating the fracture is shown in Figure 5.6.1.

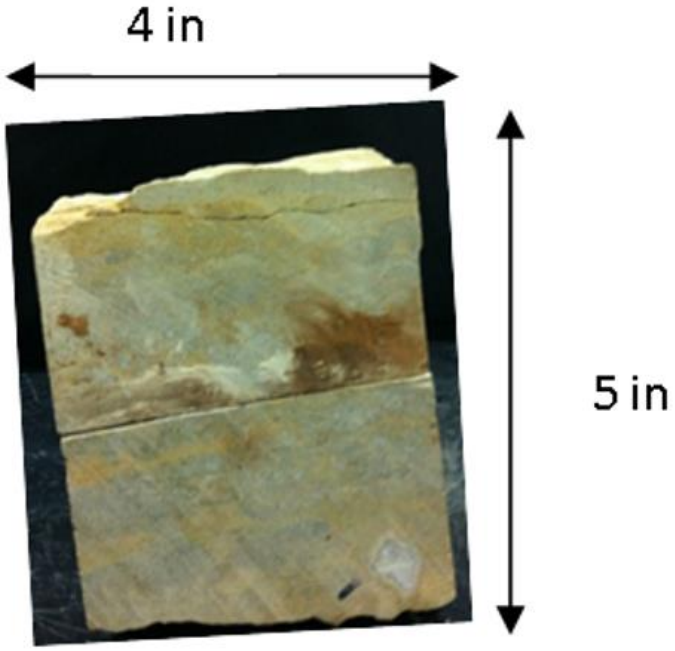

Figure 5.6.1 Fractured Rock Sample

Quick-drying cement was used for the cementing of sample inside the shear ring. A 1:3 water-cement ratio was used for the cementing purpose. One half of the rock sample was placed inside the bottom shear ring and was positioned at the desired location using molding clay. Cement slurry is poured around the sides of the rock sample in the bottom shear ring to within a few millimeters from the top which can be seen from Figure 5.6.2.

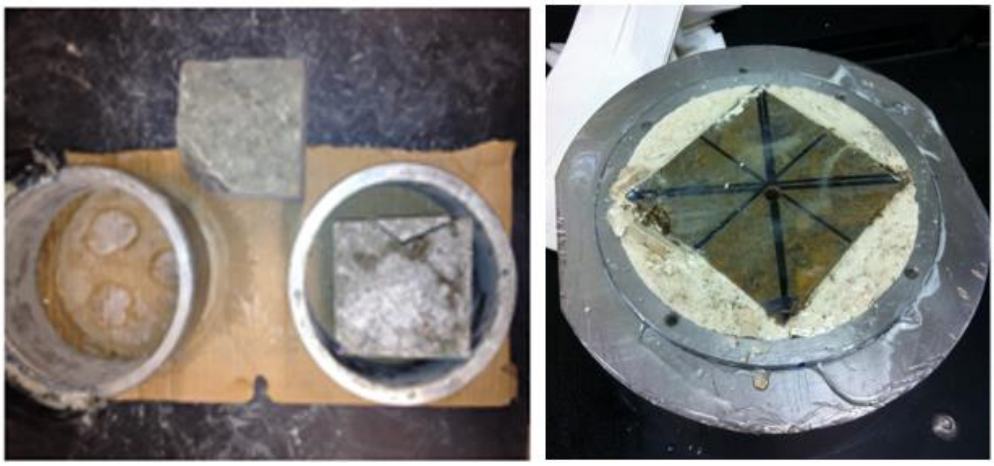

Figure 5.6.2 Cementing of the rock sample

The following test procedure was followed. First the cement slurry is allowed to set for 4-5 hours. Then the sealant material is placed on the surface of this sample. Once complete, the other half of the sample is placed on top of this sealant material to seal both samples together. Then the two halves of the spacer rings were placed on the top of the bottom shear ring. The gap is then filled using the molding clay so that the cement slurry does not go inside the sealed fracture which can be seen in Figure 5.6.3. An upper ring is fully tightened by the holding screws after it is placed on the spacer ring. Then another batch of cement slurry was poured on the top of the molding clay filling the upper specimen within a few millimeters from the top. The cement is allowed to cure to gain its full strength. Finally a spacer bars are removed after the cement is fully cured and the rock sample is ready for the testing which can be seen Figure 5.6.4.

Figure 5.6.3 Rock sample in shear ring

Figure 5.6.4 Shear ring without spacer

5.7 DIRECT SHEAR TESTING SYSTEM

The GCTS Direct Shear Apparatus is able to test a wide range of rock mechanics specimen to determine the shear strength of the fractures in the rocks. The system works on the application of normal load and horizontal shear load. The normal and shear deformations are monitored using either linear variable differential transducers (LVDTs) or dial gauges. The shear load, shear deformation, normal load and the normal deformation are monitored by the GCTS CATS software, which includes inputs from them. At the end of the experiment, a shear stress vs time graph is generated from which peak and residual shear strength are determined. Shear strength is measured by the apparatus in KPa (Kilopascals). Two air/oil booster pumps are used to set the normal load and shear displacement rate. An ISCO pump attached to this shear apparatus measures the fracture permeability simultaneously with shearing. The fracture permeability was measured from the following equation:

$$k = Q\mu_w \ln(r_2/r_1)/2\pi e Hg\rho_w \quad (2)$$

Where Q is the fluid injection rate, $Hg\rho_w$ is the pressure head at the injection point, e is the conducting aperture of the fracture, μw is the dynamic viscosity of water, r1 is the radius of the injection well, r2 is the equivalent outer radius of the fracture surface. Where;

$$r_2 = \sqrt{(L_1 \times L_2)}/\pi \quad (3)$$

L1 and L2 are the lengths of the sides of the fracture surface.

$$e = \sqrt{((6Q\mu_w \ln(r_2/r_1) / (\pi Hg\rho_w))^{1/3}} \quad (4)$$

Normal load is applied from the normal actuator; shear load is applied from the shear actuator. Hydraulic/air pressure of 30:1 is used to apply normal and shear load on the rock sample. Normal pneumatic oil is used in the hydraulic pump, which is supplied to the shear actuator and normal actuator through strong rubber cables.

The system is composed of the following components:

- Normal loading mechanism
- Shear loading mechanism
- Normal and shear load detection
- Normal and shear deformation detection
- Pump system
- Direct shear sample mounting

The normal load is evenly distributed over the plane to be tested and is applied using a hydraulic mechanical system. The normal load is applied through a normal load actuator, and the normal load actuator stroke must be greater than the dilation expected during the experiment.

The shear load is also applied using a hydraulic system. The shear load is applied through a shear actuator, which is mounted on the apparatus to apply horizontal load. The load is distributed evenly along one half face of the test sample with the resultant force acting in the direction of shearing. There are also low friction devices built into the apparatus to ensure that the resistance to shear displacement is less than the shear force applied.

The normal load is monitored using the normal load cell mounted between the normal load actuator and the top of the shear box. The shear load is monitored using a shear load cell mounted between the shear load actuator and side of the shear box. The load accuracy is $\pm 2\%$ of the maximum force reached in the test.

The normal deformation is measured using a normal load sensor, which is a linear variable differential transducer (LVDT) attached at the top of the normal load cell and the swivel pipe. The shear load is measured using a shear load sensor, which is also a linear variable differential transducer (LVDT) attached to the top of the shear actuator.

Two air/oil booster pumps operate at 100 psi, and this compressed air allows the user to easily set the normal load and alter the shear deformation rate. The shear pump includes a four-way valve to easily reverse the loading direction. The values of the normal load and shear deformation are digitally displayed, and all the controlling knobs are set on an easy-to-use front panel.

Core samples for direct shear test were four inches in length, four inches in width and about five inches in height. The samples are prepared using a rock saw. The rock sample is cemented using quick-dry cement inside two, 6-inch diameter shear rings, which are capable of holding 150 mm diameter and 150 mm high rock sample. The shear ring is then placed inside the shear box for the experiment. The shear box is then subjected to the constant normal load and horizontal load with an increment of 0.05mm/second. Figure 5.7.2 shows the schematic diagram of the shear ring with the spacer after the sample was prepared.

Figure 5.7.2 Direct shear test sample

The direct shear system features electronic sensors and digital displays, which are set in front of the panel of the metal cabinet to monitor the loads and the deformations. A standard A/D automatic data acquisition with USB interface is included in the system, which automatically logs and refines test data. The USB interface connects the control panel with the computer. All the data is recorded within a CATS software. The GCTS Direct Shear Test mode program within the CATS software allows the user to directly set up and conduct the direct shear tests. The program allows for real-time determination and control of various test inputs, such as corrected area of the specimen, normal stress and shear stress. The software also enables the conductance of the tests in multiple stages like consolidation, universal stage or shear loading. The consolidation stage is used to perform the normal consolidation, universal stage is used to define different test sequence, and

finally, shear loading is used for the optimization of the shear loading. Electric sensors are attached to the system from which the program measures normal load, shear load, normal deformation and shear deformation.

The Direct Shear test is administered to find the shear strength of the rock. The step by step procedure to run the direct shear test on the lab set up is shown below:

- Dimensions of rock samples are recorded in an Excel file with the geological data. Photographs should be taken to keep record of the test progress.
- Apparatus should be set up before the experiment.
- Sample is to be properly cemented before the experiment, and the spacer bars should be removed before the shear rings are placed inside the shear box.
- Before the sample is placed inside the shear box, the screw on the top of lower shear box should be unscrewed to create the passage for the air when the sample is inserted.
- Sample should be carefully inserted into the bottom shear box using some friction reducing fluid on the sides of the shear ring. If the sample does not go in easily, a rubber hammer should be used to hit the sample very carefully from the top so that it does not break from the middle.
- Once the sample is inside the lower shear box, the screw is used to shut off the flow of air.
- The top shear box is to be lifted from the handle after unscrewing the screw at the top of upper shear box and is to be slowly lowered onto the top of shear ring.
- Friction reducing fluids are used to reduce the friction between the shear ring and the shear box and a rubber hammer is used to hit the upper shear box from the top. The screw is again used to shut off the air.
- Fracture is exposed at this time between both the shear rings.
- Pumps, apparatus and the computer are switched on once the sample is in place.
- Software is to be started, and a new project is created. All the inputs are inserted in the new project for the desired sample.
- The knobs on the front of the control panel should be checked before each experiment.

- Turn normal load knob fully counter-clockwise and the shear load fully clockwise.
- Turn normal direction control to down and shear direction control to pull.
- Pump is turned on to start the experiment.
- The swivel top is properly placed and aligned with the upper box.
- The normal load is turned clockwise to increase the normal load to the desired value.
- The normal load is maintained constant throughout the experiment.
- After all the settings in the software are done, the experiment is executed and the shear load knob is turned to the left to slowly maintain the increment of the shear load at the rate of 0.05mm/sec.
- The shear loading continues to increase until the peak and residual shear strength of the rock sample is achieved.
- The data from the test is collected and analyzed to get the shear stress vs. time graph from which peak and the residual shear strengths are obtained.
- After the experiment, the cemented rock inside the shear ring is taken out very carefully using a hammer and a chisel.

5.8 HYDRAULIC FRACTURING CELL

To test the strength of the sealed fractures, tri-axial tests were performed. This test measures the fracture pressure of the intact concrete core and compare it with the fracture pressure of fractured core sealed with the test sealant. Knowing the pressure necessary to re-open a fracture filled with a known sealant provides a guideline during CO_2 injection. Exceeding such pressures could re-open an already sealed fracture and create a leakage pathway for CO_2.

Rock fracturing (hydraulic fracturing) experiments were performed using a 4,000 psi fracturing cell (Figure 5.8.1) with fractured concrete samples with a fracture width of 0.1 inch, fracture height of 0.5 inch and a fracture length the entire length of the core. During the first phase of the experiments, confining pressure, axial load, and borehole pressure were applied simultaneously until desired confining pressure was reached. Once confining pressure and axial load satisfy the set up requirements, the second phase involved

increasing borehole pressure with drilling mud until breakdown of wellbore takes place. A repetitive sequence of fracturing experiments was conducted, including an initial fracture propagation followed by one re-opening fracture experiment after 10 minutes of initial fracture. Water and 6% bentonite mud were used as the fracturing fluid for unfractured concrete experiments. Only 6% bentonite mud was used as the fracturing fluid for fractured samples sealed with micro-cement and polymer gel. The reason why concrete cores were used is related to their ability to deliver a close representation of low permeable formations such as shale and chalk.

In order to carry out hydraulic fracture experiments a core sample was created. These experiments require cylindrical core samples made from rock slabs or by forming cement into a mold. The following procedure was followed to manufacture cylindrical cores from rock slabs. First the rock slabs must be obtained from quarry or outcrop. Then a large drill press is used with a 5 ¾" diameter coring drill bit to drill out the core's outside diameter. Next, a surface grinder is used to smooth and square core ends. Then a drill press, with a ½" drill bit, is used to create the centered wellbore hole.

Cores must be less than 9" tall due to the pressure cell height limitation. The overall height of the cell is 15", thus leaving 6" for both top and bottom caps, as well as two spacers and the overburden cap. Furthermore, once these four steps have been completed according to the mentioned requirements the core made from a rock slab would be ready to undergo the final preparation before it can be tested. In order to avoid fluid from escaping the wellbore and causing overburden losses, the top and bottom caps are cemented into place. Before the caps can be cemented onto the core, a simple cap assembly process takes place:

- Screw injection nipple into one side of the top cap
- Screw into the other side of top cap the 1 ½" casing
- Screw into the bottom cap the 1 ½" casing

After this short assembly, if the borehole does not align perfectly with the top/bottom cap, a grinding stone designed for small applications, such as a Dremel tool, could be used to enhance the borehole's diameter. Then, epoxy is used to bond the top and bottom caps to the core. The epoxy used for this purpose is the Sikadur 31 Hi Mod Gel 1:1 ratio. Place top/bottom cap with casing in upright position over the c-clamps.

Use masking tape to cover the casing hole; this will prevent excess epoxy from clogging it. Use sand paper of 120/150 grit to make a rough surface on the cap as well as on the casing, allowing a good bond between core and cap. Once both the cap and casing have been scratched with sand paper, spread epoxy onto the entire surface of cap as well as on the side of the casing. Finally, place the core onto the cap and clamp it down in steps, to allow any necessary alignment. Clean excess epoxy from sample and let cure for 24 hours. This process, which describes how to bond the cap and the core, should be repeated for the remaining cap. Cement one cap at a time.

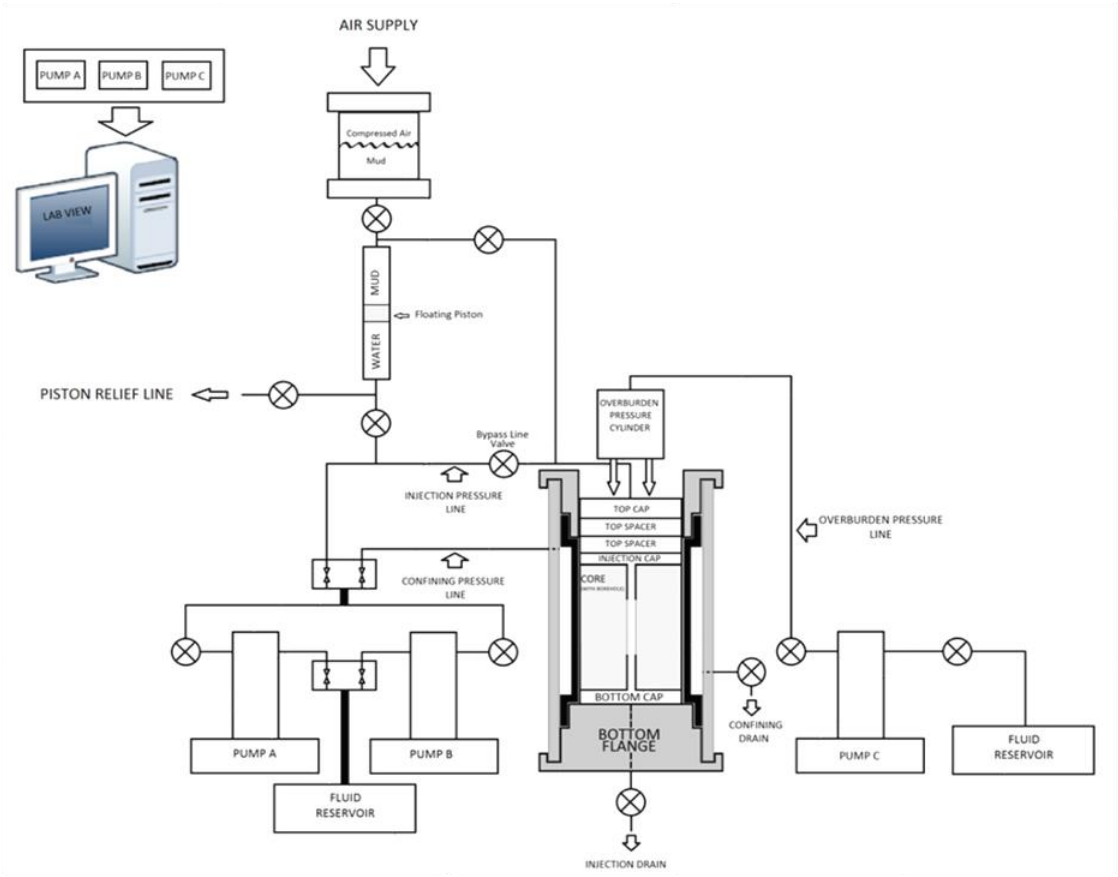

Figure 5.8.1 Hydraulic Fracturing System Schematic

High pressure (10,000 psi) low volume (100 ml) ISCO DX100 syringe type pumps are used to build up and apply pressure inside the hydraulic fracturing apparatus either for confining or fracturing purposes. The fluid that these pumps operate with is obtained from a plastic or stainless steel container used as a reservoir. Each pump has an inlet valve,

which allows fluid flow to enter the pump piston for refilling or discharging all content. Both pumps share the same inlet tubing into the reservoir, allowing refilling both pumps at the same time. The tubing used that allows fluid distribution to and from the pumps as well as into the apparatus is 1/8” and 1/4” OD stainless steel. Each pump has an outlet valve, preventing the system from depressurizing while being refilled.

A stainless steel pipe with an internal piston has been designed to accumulate and inject drilling fluids into the core sample. Syringe pumps used for this experiment were not designed to handle drilling fluids, therefore, an accumulator as shown in Figure 5.8.2, is loaded with the desired drilling mud and then by means of injecting water beneath the piston, the mud is transferred and injected into the core sample.

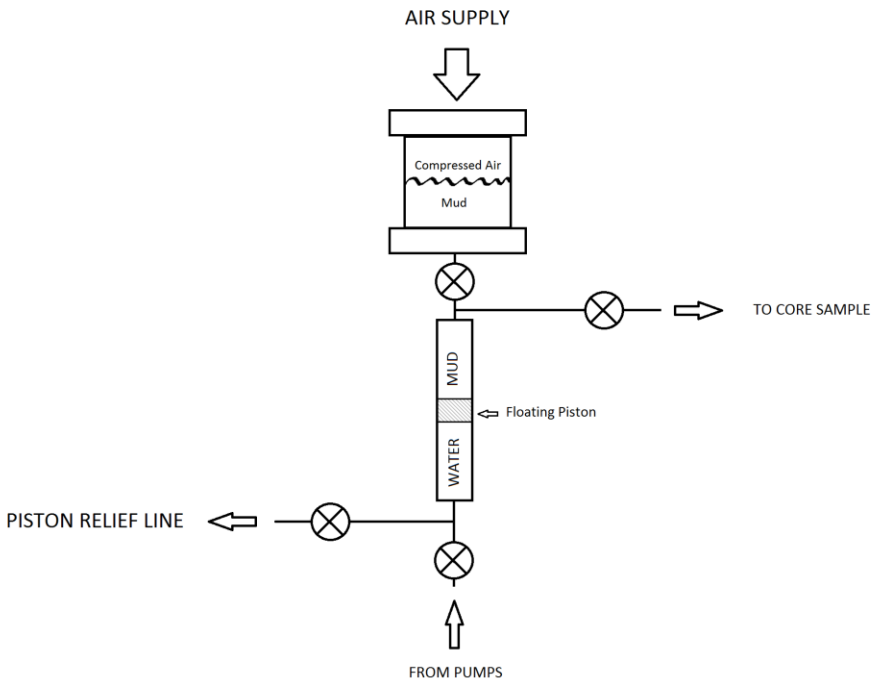

Figure 5.8.2 Mud Accumulator System

From Figure 5.8.2, it can be seen that water is delivered from the pumps to the bottom of the piston in the accumulator. Mud is transferred to the accumulator by filling a plastic cylinder and then applying compressed air to force the mud into the accumulator. Then, pressure is built underneath the piston, which displaces the mud into the core sample.

The hydraulic hand pump is connected to a piston located on the top of the apparatus frame (Figure 5.8.3). The sole purpose of this piston is to apply axial load on the top cap, thus creating overburden stress within the core.

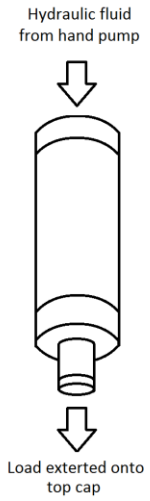

Figure 5.8.3 Overburden Piston

A pressure regulator as shown in Figure 5.8.4 is mounted in between the hand pump and the piston. It is used to bleed off hydraulic fluid in case pressure inside the piston exceeds the desired pressure.

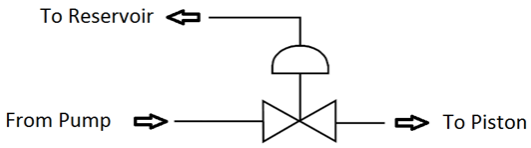

Figure 5.8.4 Bleed-Off Valve

A rubber sleeve is used to apply confining pressure inside the hydraulic fracturing apparatus. Pressure is built up in the gap between the stainless steel cylinder and the rubber sleeve. As pressure is increased, the rubber sleeve confines the core sample until the desired pressure is reached.

A stainless steel cylinder, which is placed over the rubber sleeve and rests on the bottom flange, is used as a pressure vessel to contain the highly pressurized fluid used to apply confining stresses onto the core sample. It also serves as the seat and support for the top flange.

Six all-thread rods mounted on the I-beam are used to secure and clamp down the top flange onto the stainless steel cylinder creating a seal for the rubber sleeve, which prevents leaks from the confining chamber into the upper section of the core sample.

The bottom flange, which is bolted onto an I-beam, serves as the base and foundation of the hydraulic fracturing apparatus. The bottom flange serves as a core holder, provides support for the stainless steel cylinder, and provides support for the rubber sleeve. It is important to note that the rubber sleeve is glued with clear silicone onto the core holder to avoid leaks. The bottom flange is shown in Figure 5.8.5.

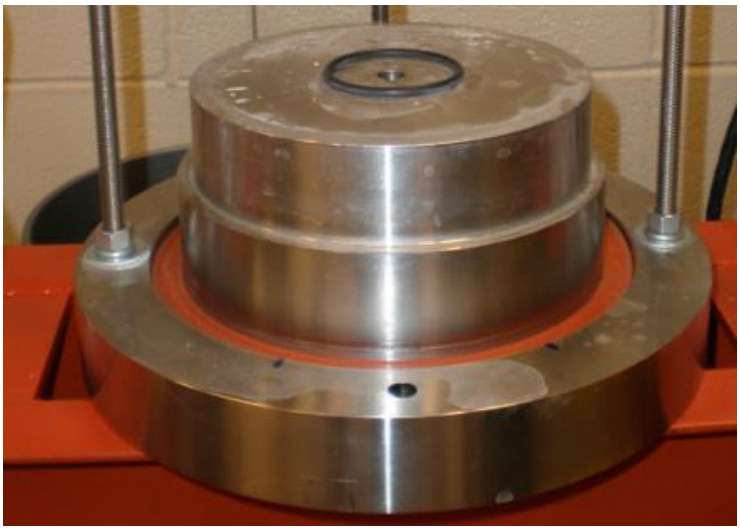

Figure 5.8.5 Bottom Flange

The top flange, shown in Figure 5.8.6, is similar to the bottom flange. It has an opening in the center so that core samples can be placed directly into the apparatus. It rests on the stainless steel cylinder and the rubber sleeve. It provides a seal between these two to avoid leakages, thus preventing confining pressure losses.

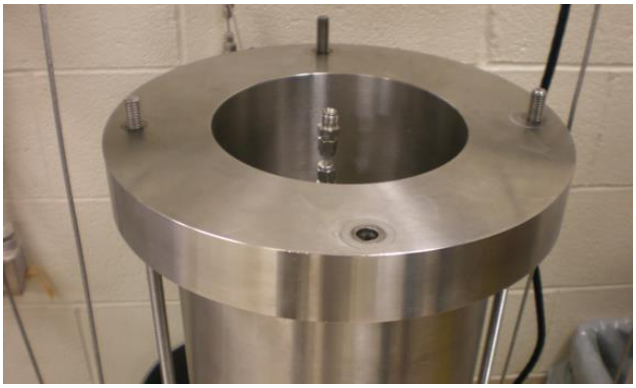

Figure 5.8.6 Top Flange

The frame, shown in Figure 5.8.7, serves as a support for the hydraulic fracturing apparatus. The bottom flange rests on an I-beam which can travel in the vertical direction by two hydraulic operated winches. The hand pump, which drives the piston mounted on the top of the frame, is located on the left side of the frame. The frame has several holes allowing the I-beam to rest at different heights.

Figure 5.8.7 Hydraulic Fracturing Apparatus

In order to start performing hydraulic fracture experiments, the accumulator valves should be set to injection mode, empty the accumulator so that no other fluid other than the

intended test fluid is found in the injection line. Place a core into the hydraulic fracturing apparatus.

Overburden and confining pressure are applied to the core before starting to run the experiment. Overburden stress is obtained by a piston pushing down on the top cap and confining pressure is applied through a rubber sleeve in the apparatus by building pressure inside of it. Fracturing fluids are prevented from escaping the bottom and top of the wellbore by placing an o-ring at the seat of the core holder and by bonding bottom and top caps to the core sample, as well as each cap having their casings cemented to the wellbore.

The accumulator mentioned above, which is mounted on the wall is used to inject the drilling mud or other hydraulic fracturing fluid only, since water is injected directly from the pumps to the core. Two gauges are located on the hydraulic fracturing apparatus. One gauge is used to control and compare injection pressure as the experiment is being run; the other gauge is used to monitor confining pressure. A computer is used to record the data as the experiment is being run by using the Isco Pump software. At this point the setup is ready for injection. Next, locate valves on the accumulator, as well as on the injection line, and set to refill. Refill the accumulator with the desired mud. Make sure the bottom exit valve is open to remove air from wellbore. Once this task is done, close the bottom exit valve and stop pumping. Open Isco Pump software to record data. For this system, head losses in the injection line are 100 psi. This should be taken into account and subtracted accordingly from the data recorded. Finally, assign a name to the file, connect the pump to the software, and start running the experiment. In between cycles, from original break down and the subsequent re-opening, the wellbore must be depressurized by opening the bottom exit valve and closing it right away.

6. RESULTS

6.1 RHEOLOGY TEST RESULTS

Table 6.1.1 shows that silica gels S2 and S3 produced similar G' readings. However, S2 did provide a noticable increase in the G″ readings (refer to Table 5.2.1 for gel formulations). For the polymer gels, the highest G' and G″ readings were generated from the M4 formulation.

Table 6.1.1 Measured Gel Strength Results

A) Gel strength versus concentration for the silica gel

B) Gel strength versus concentration for the polymer-based gel.

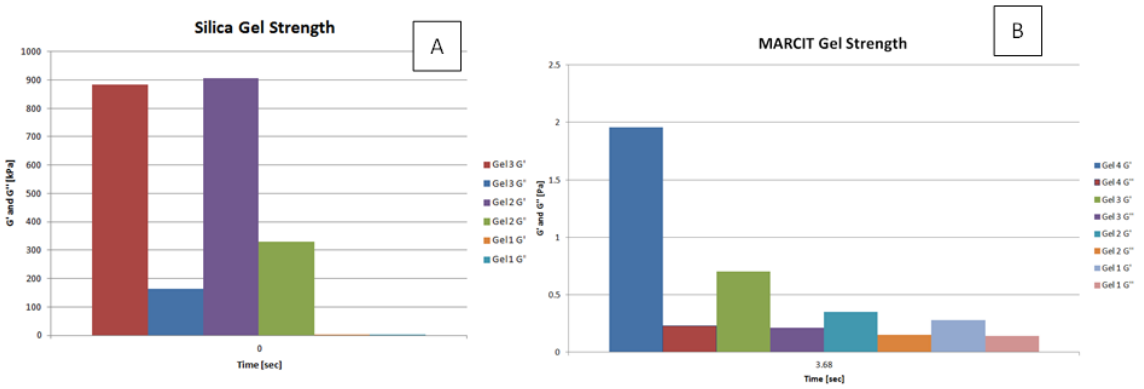

6.2 CORE FLOODING TESTS RESULTS

The final permeability results that were conducted in the core flooding apparatus are given in Table 6.2.1. The intact relative permeability was measured for all materials. The fracture permeability was measured after injecting polymer into the fracture in the Lamotte sandstone. The results show that the permeability of CO_2 is typically 5 to 10 times less than brine in a brine-filled reservoir. The same trend can be seen for the cap rock formations. Note that the residual brine concentration in the sandstone is 33% compared to 57% and 79% for the Bonneterre and Davis formations respectively. Table 6.2.1 gives the experimental results for the fracture filling plugging agent permeability tests for the Lamotte sandstone, Bonneterre dolomite, Davis, and Derby Doe Run formations. In the table, the average intact permeability for both CO_2 and KCl brine are given in the k_{before} column. K_{before} is intact permeability before sealant additive is injected into the fracture. The permeability of the sealed fracture is given in the k_{after} column. K_{after} is fracture

permeability after sealant is injected. To evaluate the effect of the plugging agent injection, the fracture sealing ratio (F_{rr}) was determined as the calculated fracture permeability divided by the measured permeability after plugging agent injection. High fracture sealing ratio (F_{rr}) indicates a more efficient plugging agent. Experimental results of fracture permeability before and after sealing agents was injected are shown on Table 6.2.1.

Table 6.2.1 Reduced Permeability Testing Matrix

Type	Name	Fluid	k_{before} [md]	R^2	Swr	Porosity	Plugging Agent	k_{after} [md]	R^2	Frr
SS	1.1	CO2	1.82	96%	0.33	16%	Marcit Polymer	3.34	99%	3,084
		KCl	5.46					12.07		853
	1.2	CO2	0.55	99%	0.33	16%	Paraffin Wax	0.15	100%	68,667
		KCl	8.36					143.08		72
	1.3	CO2	0.11	99%	0.33	13%	Silica Gel	-----	-----	-----
		KCl	5.46					4.63		2,225
	1.4	CO2	0.56	99%	0.33	17%	Marcit Polymer	0.62	99%	2,097
		KCl	26.8					4.75		274
	1.5	CO2	0.21	97%	0.34	16%	Marcit Polymer	-----	----	-----
		KCl	4.93					9.24		8,874
BT	2.1	CO2	0.002	95%	0.79	3%	Marcit Polymer	0.077	99%	133,766
		KCl	0.06					6.77		1,521
Davis	3.1	CO2	0.0004	98%	0.57	10%	Marcit Polymer	-----	-----	-----
		KCl	0.22					8.77		1,174
	3.2	CO2	0.0004	98%	0.57	10%	Cement	0.0074	97%	1,391,892
		KCl	0.22					0.248		41,532
DDR	4.2	CO2	0.00004	99%	0.39	1%	Cement	0.004	99%	2,575,000
		KCl	0.003					0.179		57,618

Of the four plugging agents tested the recorded, F_{rr} values for Marcit polymer plugging agent was between 2,077 and 133,766 for CO_2 injection (partially brine saturated with 0.5 mm fracture width), and from 274 to 8,874 for KCl injection (fully saturated with 1.0 mm fracture width). The paraffin wax F_{rr} values were 68,667 for CO_2 injection and 72 for KCl injection. The reported silica gel F_{rr} value was 2,225 for KCl injection. In contrast, the cement F_{rr} values were 1,391,892 to 2,575,000 for CO_2 injection (partially saturated with 0.5 mm fracture width) and 41,532 to 57,618 for KCl injection (fully saturated with

0.5 mm fracture width). So, for the four plugging agents tested, the fractures that were injected with cement obtained the highest F_{rr} values, thereby the greatest reduction in fracture permeability. The second highest F_{rr} values came from a fracture injected with the Marcit polymer.

When dismounting the samples from the core holder, the fractures were visually examined. It was noted that each of the plugging agents, except the cement, had issues with either worm holing or the plugging agent being completely removed from the fracture due to the increasing differential pressure.

Figure 6.2.1 shows the effect of fracture width on the polymer gels ability to seal fractures. The black bar represents the core with a 0.25 mm fracture, the dashed bar represents a 0.5 mm fractured core, and the dotted bar represents a 1.0 mm fractured core. Moving from left to right, the first group is the measured matrix permeability (core is not fractured), the middle group is the fracture permeability, and the last group is the measured permeability after the polymer plugging agent has been injected into the fractures. The polymer gel did a sufficient job reducing the flow of brine in the 0.25 mm fractured core. However, the 0.5 mm and 1.0 mm fractured cores where unable to reach their matrix permeability due to wormholes in the polymer, which were observed in the samples and reflected in the permeability results. This would suggest that the polymer is only able to withstand differential pressure for smaller fracture widths.

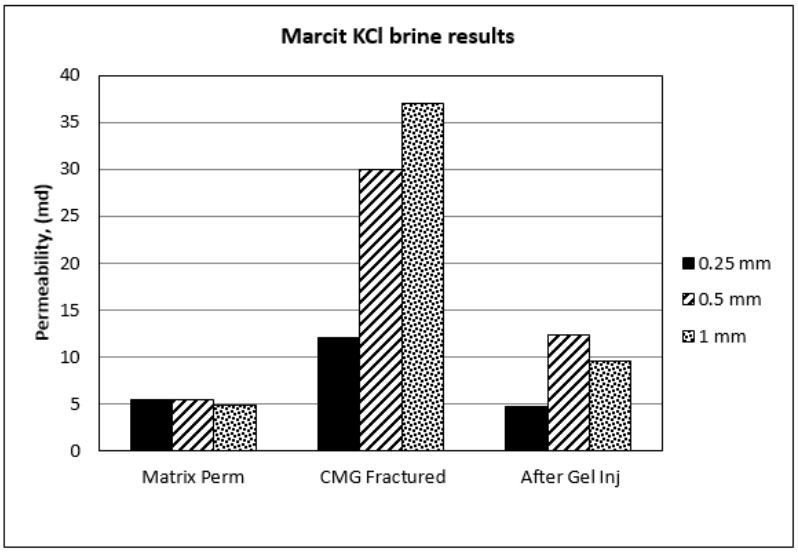

Figure 6.2.1 Fracture Permeability Results

6.3 DIRECT SHEAR STRENGTH RESULTS

The initial permeability of the fracture sealed with cement is higher than that of the polymer and the air-tight sample (Table 6.3.1). This is due to de-bonding of the cement/fracture boundary due to the application of normal and tensile stress. The smooth fracture surfaces easily led to the de-bonding of the cement/fracture boundary when stress was applied.

Table 6.3.1 Direct Shear Strength Results

Shear level	Sealing material	Permeability, (m^2)	Shear Deformation, (mm)
0%	Air	3.70512E-09	0
	Cement	6.41817E-09	0
	Polymer	3.71942E-09	0
2%	Air	3.70505E-09	6.972
	Cement	4.88743E-09	2.936
	Polymer	3.71922E-09	1.363
10%	Air	3.70489E-09	14.3
	Cement	6.41807E-09	11.771
	Polymer	3.38671E-09	9.831

The permeability of the air-tight sample was approximately constant (3.7E-9 m^2) throughout the shear deformation process. This is consistent with our expectations since the fracture surface is smooth. A similar explanation applies to the constant permeability of the polymer sample. Overall, it was observed that the smooth or non-natural state of the fractures caused an almost constant permeability value in all three samples. Sealant material did not properly bond to fracture surfaces. Thus, in subsequent experiments, a natural fracture is recommended.

Variations in fracture permeability were found with different sealing materials and different shear levels. Three different tests were performed: intact concrete sample, fractured concrete sealed with micro-cement and fractured concrete sealed with Marcit gel (Figure 6.3.1).

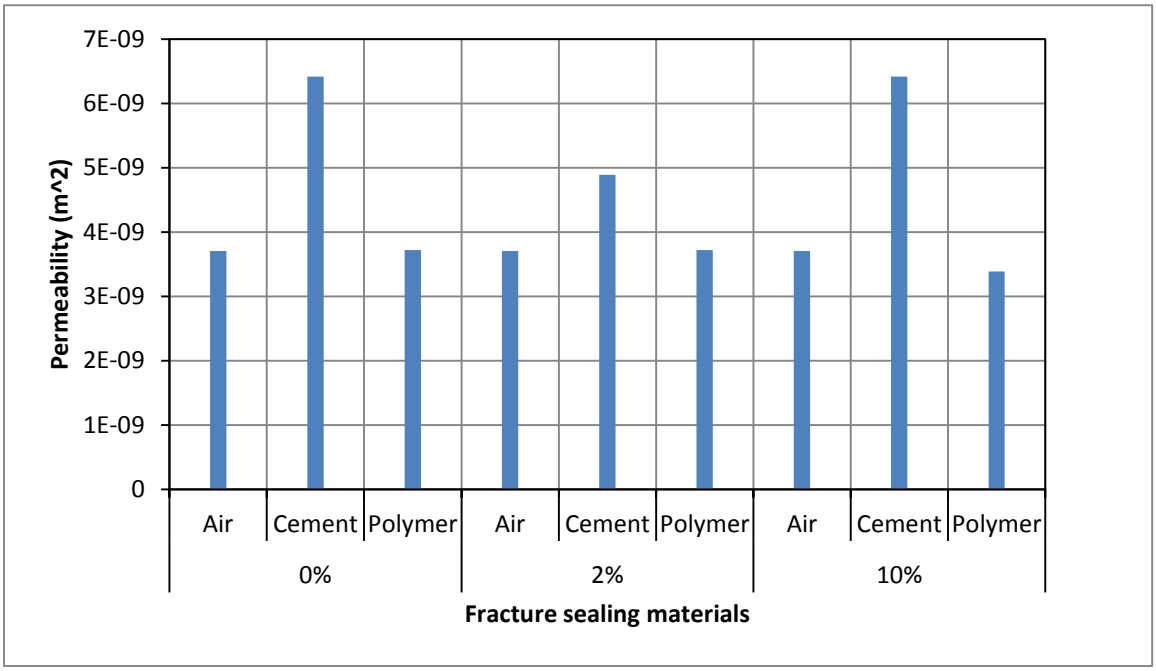

Figure 6.3.1 Fracture Permeability with Varied Shear Levels

6.4 LONG TERM STABILITY TESTS

To ensure CO_2 is stored safely over in the long-term in the reservoir, potential sealant materials need to be stable when exposed to CO_2. Marcit polymers crosslinked with chrome acetate were investigated. The various gel compositions were prepared and a semi-quantitative bottle test method used to measure gel strength. Table 6.4.1 shows gelation time with respect to concentration. Gelation was observed to occur faster in CO_2 environment than in an air environment. This could be ascribed to the quartet of lone pair electrons present in the CO_2 oxygen atoms, which facilitate ligand binding with Cr3+ crosslinker.

Stability of gel-sealed samples, exposure to CO_2, were monitored over a seven months period. Gel strength was observed to be constant over the entire test period as seen by a constant gel strength code. The various codes are described thus; C: Flowing

gel-most of the obviously detectable gel flows upon inversion; D: Moderately flowing gel-a small portion (5 to 15%) of the gel does not flow readily upon inversion; F: Highly deformable non-flowing gel-the gel does not flow to the bottle top upon inversion (reaches a point just short of bottle top); G: Moderately deformable non-flowing gel-the gel flows approximately half the way down the bottle upon inversion.

Table 6.4.2 gives the result of gel stability of CO_2 sealed samples after seven months of CO_2 exposure. At the end of seven months, no changes were observed in gel flow behavior in all samples compared to the initial flow observation for any of the gel concentrations. Hence, we conclude that gels were stable in CO_2 environment for this time period.

Table 6.4.1 Gel Set Time

	Time, hrs	4000 ppm	5500 ppm	7000 ppm	8500 ppm
No CO_2 in sample	0	A	A	A	A
	1	A	A	A	B
	1.5	B	B	D	E
	2.5	C	D	F	G
CO_2 sealed sample	0	A	A	A	A
	0.5	A	A	A	A
	1	C	D	F	G

Table 6.4.2 Long Term Gel Strength

	Gel strength code			
Time, (months)	4000 ppm	5500 ppm	7000 ppm	8500 ppm
1	C	D	F	G
2	C	D	F	G
3	C	D	F	G
4	C	D	F	G
5	C	D	F	G
6	C	D	F	G
7	C	D	F	G

The stability tests show that the polymer gels do create wormhole due to differential pressure but are chemically stable. For micro-cement the opposite is true where the cement can withstand pressure but is not chemical stable. Therefore a better approach seal off fracture might be to inject micro-cement as a primary fracture filling material with polymer gel injected as a secondary fracture filling material to avoid CO2 to get in contact with the cement.

6.5 HYDRAULIC FRACTURING RESULTS

Three different hydraulic fracturing tests were performed: intact concrete sample, fractured concrete sealed with micro-cement, and fractured concrete sealed with polymer gel (Figure 6.5.1). The samples after breakdown are presented in Table 6.5.1. An original breakdown cycle was performed injecting 6% Bentonite drilling mud. Overburden pressure was applied at 8300 psi, and confining pressure was set to 200 psi. For the un-fractured sample, the breakdown pressure occurred at 2188 psi, and re-opening pressure took place at 1856 psi. For the fractured sample sealed with micro-cement, the breakdown pressure occurred at 1100 psi, and re-opening pressure took place at 1025 psi. For the fractured sample sealed with gel, the breakdown pressure occurred at 265 psi. There was no re-opening pressure due to the weak nature of the gel sealant material. The fracture did not re-heal after original breakdown (Figure 6.5.2).

Table 6.5.1 Hydraulic Fracturing Test Results

Material	$\sigma_{2,3}$ (psi)	P_{frac} (psi)	$P_{re-open}$ (psi)	Fracture Orientation	σ_V (psi)	q (ml/min)	$\frac{\sigma_{2,3}}{\sigma_V}$
Unfractured Concrete, fractured with Water	600	2224	--	Horizontal	1037.5	50	0.58
Unfractured Concrete, fractured with 6% bentonite Mud	200	2188	1856	Vertical	8300	5	0.02
Fractured concrete sealed with Micro-cement and fractured with 6% bentonite Mud	200	1100	1025	Vertical	8300	5	0.02
Fractured concrete sealed with gel and fractured with 6% bentonite Mud	200	265	--	Vertical	8300	5	0.02

The experiment was stopped because the confining pressure started increasing, meaning that the mud was flowing through the fracture to the outside of the concrete sample. Thus, we conclude again that micro-cement is a more resistant sealant material than polymer gel. Results of hydraulic fracturing tests, measuring fracturing (P_{frac}), and re-opening ($P_{re\text{-}open}$) pressures for unfractured concrete core, fractured concrete sealed with micro-cement, and fractured concrete sealed with gel.

a) Un-Fractured concrete sample	b) Fractured sample sealed with micro-cement	c) Fractured sample sealed with polymer gel

Figure 6.5.1 Fracture Samples

Figure 6.5.2 shows breakdown and re-opening pressures for (a) unfractured concrete, fractured with water, (b) unfractured concrete, fractured with 6% Bentonite mud,

(c) fractured concrete sealed with cement, and fractured with 6% Bentonite mud, (d) fractured concrete sealed with gel and fractured with 6% bentonite mud.

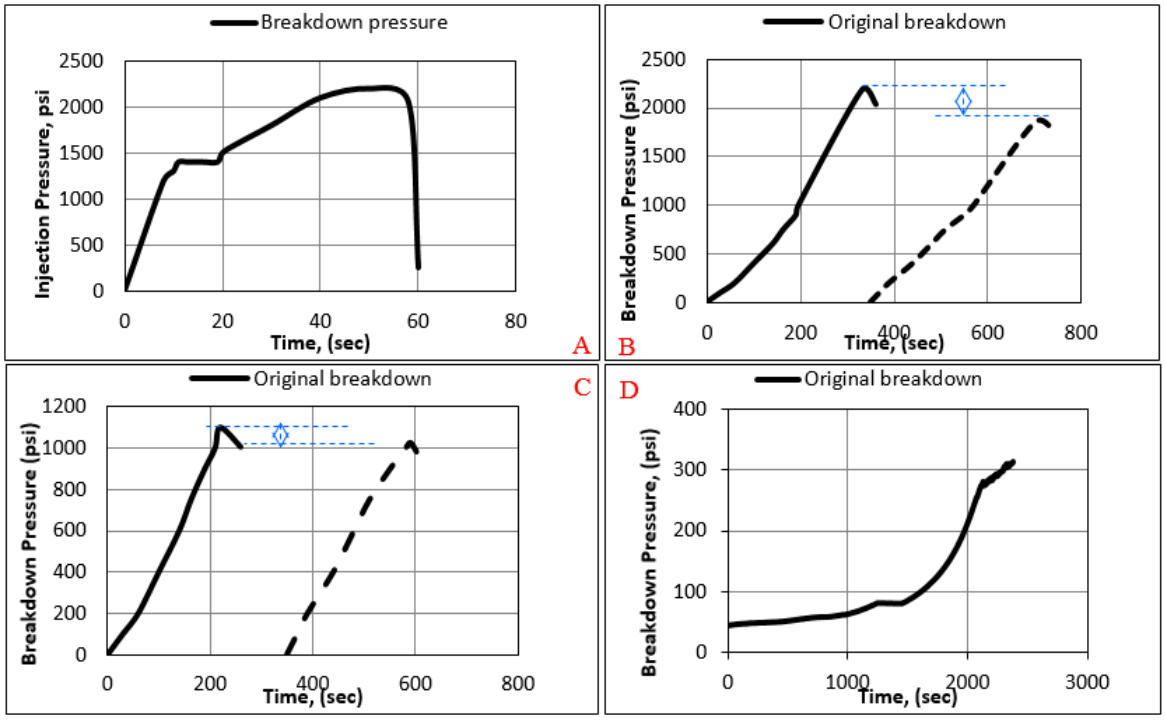

Figure 6.5.2 Breakdown Tests

7. DISCUSSION

Worm-holing seemed to be a problem for gels when the fractures get above ¼ millimeter width as observed from the experiments. The wax showed worm-holing in all tests. Only the cement did not show any tendency of the worm-holing which resulted in the best sealing efficiency of the micro-cement. Therefore it can be concluded based on these experiments that the micro-cement is the most effective sealant material tested. Since the effect of the worm-holing seems to be connected to the large differential pressure over the fracture width, a possible scenario is to inject polymer deep into the fracture and set a shallower fracture plug by using micro-cement.

So far, we have ascertained that of the four possible sealing materials, only polymer gel and micro-cement have been effective as possible sealing agents. Wax and silica did not qualify during the first two tests and have been dropped. In this test, we intend to demonstrate the effectiveness of these two materials to continuously seal fractures during periods of stress and pore pressure changes.

Re-activation of pre-existing faults occurs where the shear stress acting on the fracture plane exceeds the faults strength, which is commonly represented using the Coulomb frictional criteria (Wiprut and Zoback, 2002). When this occurs, the fault slips, and a possible leakage pathway for CO_2 is created. The essence of this study is to ascertain that, when a fracture slips, the sealant material will deform as required to continuously seal the fracture (that is prevent permeability change). To achieve this end, we designed our experiment to simultaneously measure both the shear strength and the variation in permeability of the sealed fracture with shearing. Three experiments were run on: (a) fractured rocks with no sealant material (i.e., air), (b) fractured rocks sealed with micro-cement, and, (c) fractured rocks sealed with polymer gel.

Our results show, counter-intuitively, that during the application of shear stresses, the initial permeability of the fracture sealed with cement is higher than that of polymer and air-filled (unsealed) sample. This is due to de-bonding of the cement surface-fracture surface boundary due to the application of normal and tensile stress. The smooth fracture surfaces easily led to the de-bonding of the cement-fracture boundary when stress was applied.

The permeability of the air-filled sample was approximately constant (3.75×10^6 md) throughout the shear deformation process. This is consistent with our expectations since the fracture surface is smooth. A similar explanation applies to the constant permeability of the polymer sample. Overall, it was observed that the smooth or non-natural state of the fractures caused an almost constant permeability value in all three samples. Sealant material did not properly bond to fracture surface. Further experiments in this area should be conducted on more natural fracture planes (i.e., irregular planes).

Three different hydraulic fracturing tests were performed; intact concrete sample, fractured concrete sealed with micro-cement, and fractured concrete sealed with polymer gel.

An original breakdown cycle was performed injecting 6% Bentonite drilling mud. Overburden pressure was applied at 8300 psi, and confining pressure was set to 200 psi. For the un-fractured sample, the breakdown pressure occurred at 2188 psi and re-opening pressure took place at 1856 psi. For the fractured sample sealed with micro-cement, the breakdown pressure occurred at 1100 psi, and re-opening pressure took place at 1025 psi. For the fractured sample sealed with gel, the breakdown pressure occurred at 265 psi. There was no re-opening pressure due to the weak nature of the gel sealant material. The fracture did not re-heal after original breakdown. The experiment was stopped because the confining pressure started increasing, meaning that the mud was flowing through the fracture to the outside of the concrete sample. Thus, we concluded again that micro-cement is a more resistant sealant material than polymer gel.

Of the four candidate sealing materials, only the polymer gels were tested for long-term chemical stability under exposure to CO_2. Wax and silica were not studied because wax would not be thermally stable under CO_2 storage reservoir conditions. As mentioned above at the end of seven months, no changes were observed in gel flow behavior in all samples compared to the initial flow observation for any of the gel concentrations. The gel mechanical strengths were the same as at the beginning of the measurements. Hence, we conclude that gels were stable in CO_2 environment for this time period.

This stability test shows that, although the polymer gels create wormholes due to differential pressure, they are however chemically stable. For cement the opposite is true. For Portland based micro-cement, the cement can withstand large pressures but is reported

to not be chemically stable (Shen and Pye, 1989, Kutchko et al., 2007, Bachu and Bennion, 2009). These studies observed that cement is not chemically stable when exposed to CO_2 over a long period due to carbonation, in which CO_2 reacts with calcium hydroxide found in cement and causes its degradation and porosity increase. This study investigated calcium aluminate cement where a similar carbonation process occurs with exposure to supercritical CO_2 however, in these cements, the porosity and strength was not significantly changed with CO_2 exposure (Fernandez-Carrasco et al 2008).

For Portland based cements, a plausible approach to seal-off fractures might be to inject micro-cement as a primary fracture-filling material with polymer gel injected as a secondary fracture filling material to avoid CO_2 contact with the cement.

8. CONCLUSIONS

In this thesis, a novel methodology consisting of a series of modified experimental apparatuses to screen sealing materials for CO_2 leakage through fractures has been developed. A set of paraffin wax, silica-based gel, polymer-based gel, and micro-cement have been studied to investigate their ability to effectively seal CO_2 injection induced fractures of widths from ¼ mm up to 1mm. Based on the experiments run, the following conclusion can be drawn:

- The experiments showed that all sealant materials significantly reduced the fracture permeability. However, the micro-cement (55% wt) was the most effective sealant agent and was the only sealant that was able to withstand the large differential pressure caused by CO_2 or brine injection pressure which caused wormholes to occur in the wax and gel sealants. The Marcit gel with a polymer concentration between 4000 ppm to 8500 ppm is not effective in sealing fractures with widths greater than 1mm. However, if fracture width is smaller than 1mm, weak gel might work.
- The stability evaluation of the fracture sealing materials showed that the polymer gel is stable when exposed to CO_2.
- All four sealant materials (paraffin wax, silica gel, marcit gel and micro-cement) were able to seal the fracture and reduce fracture permeability. However, none of these sealant materials were able to get the strength of the sealed-sample to that of the original in-tact sample. The breakdown pressure of the intact sample is 2188 psi. The closest value to this is 1100 psi for samples sealed with micro-cement.
- During shear testing, the permeability of the sealed fractures were almost constant for all three sealant materials. This was due to the very smooth surfaces of the fractures. This caused de-bonding to occur between sealant material and fracture surface. For further evaluation, we recommend the usage of natural or non-smooth fractures.
- Samples sealed with micro-cement had a higher breakdown pressure (1,100 psi) than samples sealed with gel (314 psi). Thus, micro-cement seal strength out

preformed the gel. Therefore, micro-cement is the recommended sealant material for CO_2 leakage pathways.

- Future work for this project should include evaluating multiple sealing materials pumped in stages. For example, inject polymer gel followed by cement.

REFERENCES

Ahmad, R.S. A., Meysam N., Ali Emadi, M., Narges, J.E., 2010. Analytical and experimental study to predict the residual resistance factor on polymer flooding process in fractured medium. Transport in Porous Media. 85, 3, 825-840.

Bachu, S., Bennion, B., 2009. Experimental assessment of brine and/or CO2 leakage through well cements at reservoir conditions. International Journal of Greenhouse Gas Control. 3, 4, 494-501.

Bai, B., Li, Y., Liu, X., 1999. New development of water shutoff and profile control in oilfields in China. Oil Drilling & Production Technology, 20, 3.

Bai, B., Li, L., Liu, Y., Wang, Z., Liu, H., 2004. Preformed particle gel for conformance control: Factors affecting its properties and applications. SPE 89389-MS paper presented at the SPE/DOE Symposium on Improved Oil Recovery. Tulsa, Oklahoma, April 17-21.

Bai, B., Li, L., Liu, Y., Liu, H., Wang, Z., You, C., 2007a. Preformed particle gel for conformance control: Factors affecting its properties and applications. SPE Reservoir Evaluation & Engineering. 10, 4, 415-422.

Bai, B., Liu, Y., Coste, J.P., Li, L., 2007b. Preformed particle gel for conformance control: Transport mechanism through porous media. SPE Reservoir Evaluation & Evaluation 2007, 10, 176.

Bai, B., Huang, F., Liu, Y., Seright, R.S., Wang, Y., 2008. Case study on preformed particle gel for in-depth fluid diversion. Paper SPE 113997 presented at the SPE/DOE Symposium on Improved Oil Recovery, Tulsa, April 19-23.

Barlet-Gouédard V., Rimmelé G., Goffe, B., and Porcherie, O., 2006. Mitigation strategies for the risk of CO2 migration through wellbores. SPE paper 98924. Proceedings of the 2006 IADC/SPE Drilling Conference, Miami Florida, February 21-23.

Benjamin, C., Karl W.B., Michael, A.C., Thomas, A.B., Jan, M.N., Nordbotten, M.D., Adam, J., 2012. Initial evaluation of advantageous synergies associated with simultaneous brine production and CO2 geological sequestration. International Journal of Greenhouse Gas Control. 8, 90-100.

Benson, S.M., Hepple, R., 2005. Prospects for early detection and options for remediation of leakage from CO2 storage projects. Carbon dioxide capture for storage in deep geologic formations, volume 2, D.C. Thomas and S.M. Benson (eds.), 2005 Elsevier Ltd.

Bert M., Ogunlade, D., Heleen de C., Manuela, L., and Leo, M (Eds). 2005. Carbon dioxide capture and storage. A Special Report of Working Group III of the Intergovernmental Panel on Climate Change,IPPC, Geneva,Switzerland, pp. 53.

Celia, M.A., Bachu, S., Nordbotten, J.M., Gasda, S.E., Dahle, H.K. 2005. Quantitative estimation of CO2 leakage from geological storage: Analytical models, numerical models, and data needs. Proceedings, 7th International Conference on Greenhouse Gas Control Technologies, 5-9 September 2004, Vancouver, Canada, pp. 663 –671, Elsevier Ltd., 2005.

Department of Energy, National Energy Technology Laboratory. NETL/DOE-2009/1389. Current and future technologies for gasification-based power generation. A pathway study focused on carbon capture advanced power systems R&D using bituminous coal-volume 2, November 2009.

Goodarzi, S., Settari, A., Keith, D., 2012. Geomechanical modeling for CO2 storage in Nisku aquifer in Wabamun lake area in Canada. International Journal of Greenhouse Gas Control, 10, 113-122.

Gutierrez, M., Øino, L.E., Nygaard, R. 2000. Stress-dependent permeability of a de-mineralised fracture in shale. Marine and Petroleum Geology, V17, 895-907.

Jens, T. B., Abdullah, C., Quanlin, Z., 2012. Impact-driven pressure management via targeted brine extraction - conceptual studies of CO2 storage in saline formations. International Journal of Greenhouse Gas Control. 7, 168-180.

Khan, F., Husain, T., Hejazi, R., 2004. An overview and analysis of site remediation technologies. Journal of Environmental Management. 71, 2, 95-122.

Kuskraa, V., Godec, M., 2007. IEA greenhouse gas R&D programme. Remediation of leakage from CO2 storage reservoirs 2007/11.

Kutchko, B.G., Strazisar, B.R., Dzombak, D.A., Lowry, G.V., Thaulow, N., 2007. Degradation of wellbore cement by CO2 under geologic sequestration conditions. Environ Sci. Technol. 41, 4787-4792.

Liteanu, E., Spiers, C.J., 2011. Fracture healing and transport properties of wellbore cement in the presence of supercritical CO2. Chemical Geology. 281, 3-4, 195-210.

Mahendra, S., Anil, R., Bhawani, S., 2011. Modified Mohr-Coulomb criterion for non-linear triaxial and polyaxial strength of intact rock. International Journal of Rock Mechanics and Mining Sciences, 48, 4, 546-555.

Michael, K., Arnot, M., Cook, P., Ennis-King, J., Funnell, R., Kaldi, J., Kirste, D., Paterson, L., 2009. CO2 storage in saline aquifers I - current state of scientific knowledge. Energy Procedia, 1, 1, 3197-3204.

Min, Z., Bachu, S., 2011. Review of integrity of existing wells in relation to CO2 geological storage: What do we know? International Journal of Greenhouse Gas Control. 5, 826-840.

Shen, J., Pye, D., 1989. Effects of CO2 attacks on cement in high temperature applications. SPE/IADC 18618, presented at SPE/IADC drilling conference, New Orleans, LA, February 28- March 3.

Sydansk, R.D., 1988. A new conformance-improvement-treatment chromium (III) gel technology. SPE 17329-MS paper presented at the SPE Enhanced Oil Recovery Symposium, Tulsa, OK, April 16–21.

Tongwa, P., Nygaard, R., Bai, B., 2013. Evaluation of a nanocomposite hydrogel for water shut-off in enhanced oil recovery Applications: design, synthesis, and characterization. Journal of Applied Polymer Science, 128, 787-794.

Watson, T.L., Bachu, S., 2008. Identification of wells with high CO2 leakage potential in mature oil fields developed for CO2 enhanced oil recovery. SPE 112924-MS paper presented at the SPE/DOE Symposium on Improved Oil Recovery, Tulsa, OK, April 20–23.

Wiprut, D., Zoback, M.D., 2002. Hydrocarbon Seal Quantification edited by A.G. Koestler and R. Hunsdale. NPF Special Publication 11, pp. 203-219, Published by Elsevier Science B.V., Amsterdam. © Norwegian Petroleum Society (NPF), 2002.

Youn-Kyou, L., Pietruszczak, S., Byung-Hee, C., 2012. Failure criteria for rocks based on smooth approximations to Mohr-Coulomb and Hoek-Brown failure functions. International Journal of Rock Mechanics and Mining Sciences, 56,146-160.

Zhang, Y., Oldenburg, C., Benson, S.M., 2004. Vadose zone remediation of carbon dioxide leakage from geologic carbon dioxide sequestration sites. Vadose Zone Journal, 3, 3, 858-866.

VITA

Aaron Jeffrey Blue received his Bachelor of Science in Petroleum Engineering from Missouri University of Science and Technology in December 2009. In January of 2010 Aaron enrolled in the Petroleum Engineering Master degree at the same university. In November 2011, Aaron was hired by a drilling fluid company as a Research Engineer. Aaron received his Master of Science in Petroleum Engineering from Missouri University of Science and Technology in May of 2016.